Article

Evaluation of *In-Vitro* Release Kinetic and Mechanisms of Curcumin Loaded-Cockle Shell-Derived Calcium Carbonate Nanoparticles

Maryam Muhammad Mailafiya [1,2]*, Kabeer Abubakar [1,2], Abubakar Danmaigoro[3], Samaila Musa Chiroma[1,4], Ezamin Bin Abdul Rahim[5], Mohamad Aris Mohd Moklas[1]* and Zuki Abu Bakar Zakaria[6].

1 Department of Human Anatomy, Faculty of Medicine and Health Sciences, University Putra Malaysia, 43400 Serdang, Selangor Darul Ehsan, Malaysia; kabeernakhadee@yahoo.com (K.A.); musasamailachiroma@yahoo.com (S.M.C.)
2 Department of Human Anatomy, College of Medical Sciences, Federal University Lafia, 950101, Akunza, Lafia, Nasarawa State, Nigeria
3 Department of Veterinary Anatomy, Faculty of Veterinary Medicine, Usman Danfodiyo University, 840213, Sultan Abubakar,, Sokoto State, Nigeria; abubakar.danmaigoro@udusok.edu.ng (A.D.)
4 Department of Human Anatomy, Faculty of Basic Medical Sciences, University of Maiduguri, 600230, Maiduguri, Borno State, Nigeria.
5 Department of Radiology, Faculty of Medicine and Health Sciences, University Putra Malaysia, Serdang 43400, Selangor Darul Ehsan, Malaysia; ezamin@upm.edu.my (E.B.A.R.)
6 Department of Preclinical Sciences Faculty of Veterinary Medicine, University Putra Malaysia, Serdang 43400, Selangor Darul Ehsan, Malaysia; zuki@upm.edu.my (Z.A.B.Z)

* Correspondence: aris@upm.edu.my (M.A.M.M.); Tel.: +60193387042 and maryam.mailafia@gmail.com (M.M.M.); Tel.: +60182018457.

First Author's ORCID: http://orcid.org/0000-0003-1734-2288

Abstract: Curcumin has restrained clinical applications due to poor bioavailability. This study aimed to synthesize cockle shell-derived calcium carbonate (aragonite) nanoparticles ($CSCaCO_3NP$) for delivery of curcumin and to evaluate its kinetic release *in vitro*. $CSCaCO_3NP$ was synthesized and conjugated with curcumin (Cur-$CSCaCO_3NP$) using a simple top down approach and characterized for its physicochemical properties as a potential curcumin carrier. *In vitro* release profile was assessed using dialysis bag membrane method. The release data were fitted to Korsmeyer-Peppas, Zero order and Higuchi models to evaluate the mechanism of release pattern. A spherical shaped $CSCaCO_3NP$ with a surface area of 14.48±0.1 m^2/g, average mean diameter size of 21.38±2.7 nm and a zeta potential of -18.7 mV was synthesized which has a high loading content and encapsulation efficiency. The FT-IR and XRD revealed less observable changes on the peaks after conjugation. *In vitro* kinetic release profile demonstrated sustained release and best fitted to the Higuchi equation model. The results of this study showed the capacity of the synthesized $CSCaCO_3NP$ to encapsulate curcumin efficiently with a stable release *in vitro*. This could give an insight and supportive ideas on the potentials of $CSCaCO_3NP$ for curcumin delivery. Therefore, $CSCaCO_3NP$ holds future prospects in preclinical framework to enhance curcumin efficacy for oral therapeutic applications.

Keywords: Cockleshell; Nanoparticles; Curcumin; Aragonite; Therapeutics; Kinetic release.

1. Introduction

 doi:10.20944/preprints201908.0254.v1

Over the last few decades, sequential encroachment of nanotechnology in the field of biomedicine for development of therapeutic agents is gaining continuous beneficial impact in scientific research [1–4]. The advanced interdisciplinary field of research have appeared a forward-thinking division of sciences, traversing across many fields of research including engineering, agricultural science, cosmetics, food science and technology, biology, biomedical sciences and pharmaceutical sciences [5]. The rapid burgeoning multidisciplinary field of nanomedicine spread across sciences with outstanding efficiency in manipulating bulk biogenic materials ranging from extremely small to bigger dimensions on nanoscales [6].

Curcumin (diferuloylmethane) is a yellow nontoxic highly potent biological active substance that is isolated from rhizome of turmeric (*Curcuma longa L.*) that belongs to the ginger family (*Zingiberaceae*) [7,8]. It possesses numerous health benefits with regard to its potent medicinal values, great pharmacological effects as well as wide safety margin, yet posed with some limitations concerning poor bioavailability when administered orally due to its insolubility and rapid degradation in alkaline pH environment [7]. It is one among the insoluble therapeutic agents that presents poor bioavailability when orally administered [9]. In addition, high percentage of curcumin is digested easily at the gastro intestinal tract (GIT) due to rapid metabolism resulting into high amount of curcumin being excreted leaving behind only few traces [10]. Approximately 70% of discovered drugs and medicinal plants candidates are poorly soluble. About 40% of the oral immediate-release (IR) drugs and many herbs are practically insoluble as documented in previous literatures [11,12]. The poor oral bioavailability emanating from insoluble drugs possesses some recurrent difficulties in drug research and developments. Frequent paucity in the effectiveness of orally administered drugs resulting to poor bioavailability is generally because of dissolution-limited absorption by the body [12,13]. Usually high dose of curcumin is required to overcome such conditions thereby maximizing it's concentration in the blood to be of equal range with the therapeutic blood concentration [12,14]. These setbacks has led to curcumin's major drawbacks as a standard therapeutic agent [15,16]. However, curcumin being safe and highly efficacious could be protected from direct contact with the gastrointestinal contents via direct uptake by the cells, boycotting fast metabolism and rapid chemical degradation [8]. Thus, Encapsulation within delivery vehicles to obtain a sustained release and maximum absorption of curcumin at the upper gastrointestinal tract could be achieved since drug delivery system holds a good prospect in oral drug administration [8,9,16].

Cockle shell is a shell of marine bivalve mollusk that is also known as *Anadara granosa.* It is a biogenic inorganic material that is cheap, readily available and decomposes slowly due to its strong composition properties [17]. It is well documented as an excellent source of abundant pure calcium carbonate in aragonite polymorphic form [18]. Nanocarriers are certainly the most valuable functional building blocks and the most relevant tools in nanomedicine [19]. In fact, the everlasting interactions between research on biogenic nanocarriers and biomedicine has led researchers in the field of nanomedicine to synthesize inorganic calcium carbonate nanoparticle from naturally abundant cockle shell material for the delivery of therapeutic agents [20].

Calcium carbonate ($CaCO_3$) is one of the most versatile natural material extracted either by mining from earth crust or synthesized in laboratories from seashells using different standard methods of production [21]. It could be emphasized that CS-$CaCO_3$NP have received much attentions considering its potential ability to enhance therapeutic index of drugs, increases physical stability and minimization of drug's side effect in the body [22,23]. In addition, CS-$CaCO_3$NP has proven promising effective use for drug delivery probably due to its surface structural porosity, high loading capacity, response to pH degradation, numerous functional group endings for electrostatic ion bonds and high surface area [22]. The applications of this biogenic inorganic carrier were reported in some pioneered works on a successful targeted delivery of drugs for cancer therapy and chemoprevention[23–25]. Notwithstanding the fact that its safety level was demonstrated using

human breast cell line, osteoblastic and osteogenic cell lines for its biocompatibility [20,23,25,26] and in animal models [27,28]. Hence, the synthesis and use of biogenic inorganic cockle shell derived calcium carbonate for curcumin delivery with the ability to boost its therapeutic efficacy is essential. There are several nanocarriers currently in use for curcumin delivery which demonstrated the enhanced bioavailability and solubility, these carriers includes; Silk fibroin [29], Chitosan [30], fibrinogen [31], Polymer [32], Solid lipid nanoparticle [33], Micelles [8] and Cassava starch nanoparticles [34]. To the best of our knowledge, no studies have yet demonstrated the usefulness of cockle shell-derived calcium carbonate (aragonite) nanoparticles for curcumin delivery.

The present study aimed to synthesize and evaluate the *in vitro* kinetic release mechanisms of Cur-CSCaCO$_3$NP. The development of CSCaCO$_3$NP as a potential nanocarrier for curcumin delivery was conducted using simple top down method. Loading of curcumin onto CSCaCO$_3$NP was carried out using simple precipitation method, followed by the characterization of the physicochemical properties of free curcumin, CSCaCO$_3$NP and Cur-CSCaCO$_3$NP using standard techniques. Curcumin *in vitro* kinetic release pattern and mechanism from CSCaCO$_3$NP was evaluated using the dialysis bag membrane method and the release data were fitted into different equation models. The size and shape of the synthesized CSCaCO$_3$NP were adequate for delivery of curcumin. Cur-CSCaCO$_3$NP demonstrated adequate prolong, steady and substantial release regardless of the difference in the pH of the environment. The surface charge and large surface area obtained for the nanoparticles promoted good loading capacity and encapsulation efficiency, which led to sustained release of curcumin indicating a fair stability of the nanocarrier.

2. Materials and Methods

2.1. Chemical and Reagents

The cockle shells used were purchased from a local wet market in Malaysia. Curcumin, Phosphate buffer saline (PBS) from Sigma Aldrich St. Louis Co., United State. Dodecyl dimethyl betaine (BS-12) was obtained from Sigma-Aldrich (Steinheim, Germany) and Dialysis bag membrane (10kDA USA). Further, Ethanol was obtained from Apical Scientific Sdn, Bhd Malaysia and bleaching agents from Bleach liquor, India. All other reagent and chemicals used were of analytical grade.

2.2 Preparation and Development of Micron Size Cockle Shell Powder

The previous method was adopted in this study for the preparation of micron size CaCO$_3$ nanoparticles with little modifications [22]. Briefly, 250 g of cockle shells were washed thoroughly in a running tap water to get rid of dirt and stains. They were boiled in a steel container, rewashed in a liquid containing 100 ml of water and 25 ml of Bleaching agent (Bleach liquor, India) at the ratio of 3:1, and scrubbed with a hard brush to remove the remaining stains and debris from the shells. The shells were oven dried (Memmert UM 2500, Germany) at 50 °C for two weeks. The dried cockle shells were grounded using a rotary pulverizing blending machine (RT-08 rpm 2500, Taiwan) into fine powder particles. The fine particles were sieved using a stainless laboratory test sieve with an aperture size of 90 µm followed by a smaller pore sized sieve of 75 µm (Endecott Ltd., London, England) finally the micron size CSCaCO$_3$ fine powders was stored in an oven at 50 °C for further analysis.

 doi:10.20944/preprints201908.0254.v1

2.3 *Synthesis of $CaCO_3$ Nanoparticles from Micron-Sized Cockle Shell Powder*

Synthesis of cockle shell $CaCO_3$ nanoparticles was carried out using a top-down method by mechanical milling [22]. 2 g of 75 um micron sized cockle-shell $CaCO_3$ fine powder was mixed with 50 ml of deionized water to make an aqueous solution in a flat bottom flask of which 0.5 ml of dodecyl dimethyl betaine (BS-12) was added to the solution, a magnetic stirring bar was dropped in the solution beaker to promote the stirring process and were placed on a Systematic Multi-Hotplate Stirring machine (Systematic Multi-Hotplate Stirrers 6 Positions, Wise Stir® Korean) stirring at 1000 rpm at 27 °C for 3 hrs after which the aqueous solution was filtered with a filter paper (Filter, Fiorina, China). Repeated rinsing of the surfactant (BS-12) from the resultant sediments was achieved by continuous rinsing with deionized water until a surfactant (BS-12) free nanoparticles were obtained after which it was allowed to dry in oven at 50 °C for 3 days. The synthesized nanoparticles were further placed and sealed with seven ceramic balls in a cylindrical iron jar that has a diameter of 8 cm. It was then rolled on the roller mill machine for 8 days at 200 rpm. Finally, fine $CSCaCO_3$NP were obtained, packaged in a glass bottle and stored at 50 °C in an oven for later use.

2.4 *Loading of Curcumin onto $CSCaCO_3$NP*

The loading of Curcumin onto $CSCaCO_3$NP was carried out according to the methods described in previous literatures with slight modifications [25,29]. Briefly, six (6) formulations of Cur-$CSCaCO_3$NP with different ratios of nanoparticles to curcumin were analyzed (Table 1). Each sample of the weighed curcumin was dissolved in 1 ml of ethanol followed by 5 ml of deionized water and then vortexed for 2 mins (3 times) with 15 secs resting intervals after which the individual samples of curcumin solution were mixed with $CSCaCO_3$NP respectively. The mixtures were stirred on a Systematic Multi-Hotplate Stirring machine (Systematic Multi-Hotplate Stirrers 6 Positions, Wise Stir® Korean) with a magnetic bars placed in each solution to enhance the mixing process. The stirring process took place in a dark room over night at 200 rpm. The resultant solutions were ultra-centrifuged at 20,000 rpm for 20 min at 4 °C (Optima XPN, Beckman Coulter instruments Inc., CA, USA). After which each solutions were washed twice with 5 ml of deionized water to remove the excess ethanol and remaining curcumin that were not encapsulated. Finally, the samples were freeze-dried and crushed into fine powder again.

Table 1. Formulations of Cur-$CSCaCO_3$NP with different ratios of nanoparticles to curcumin.

CODE	$CSCaCO_3$NP (mg)	CURCUMIN (mg)	RATIO
1	20	30	2:3
2	20	20	1:1
3	20	10	2:1
4	10	30	1:3
5	10	20	1:2
6	10	10	1:1

 doi:10.20944/preprints201908.0254.v1

2.5 *Curcumin Loading Capacity (LC) and Encapsulation Efficiency (EE)*

The loading capacity and encapsulation efficiency of $CSCaCO_3NP$ on curcumin were determined by substituting the difference between the total amount used to prepare the nanoparticles and the amount of compound present in the aqueous phase after ultra-centrifugation per weight of the $CaCO_3NP$. Thus, loading capacity was calculated by dividing the weight of the total encapsulated drug in nanoparticles by the total weight of the nanoparticles, which is expressed in percentage. It is the total amount of drug delivered per amount encapsulated [22]. Encapsulation efficiency is the total amount of drug entrapped or loaded per unit of the initial weight of the nanoparticles, which is expressed in percentage. It gives the exact amount of the drug entrapped by the nanocarrier after loading [25]. Weight of the total drug entrapped was determined by subtracting the weight of the total drug fed from weight of the non-encapsulated drug or unfed drugs (total weight of the drug fed-total weight of the unfed drug). The amounts of the free curcumin in the supernatant was determined by measuring the absorbance at a maximum wavelength of 430 nm via spectrophotometry (PerkinElmer Lambda 35 Boston, MA, USA). Data were obtained by measuring the samples in triplicates and average mean values were taken. The loading efficiency and encapsulation efficiency (EE) were calculated by the following equation (1) and (2) below respectively:

$$\text{Loading Content (LC \%)} = \frac{W_t - W_f}{W_{Np}} X\ 100 \quad \ldots (1)$$

$$\text{Encapsulation Efficiency (EE \%)} = \frac{W_t - W_f}{W_t} X\ 100 \quad \ldots (2)$$

Note: W_t = Total weight of drug fed, W_f = Total weight of the non-encapsulated drug (free drug), W_{NP} = Weight of the nanoparticles.

2.6 *Characterisation of $CSCaCO_3NP$ and Cur-$CSCaCO_3NP$*

Physicochemical properties of $CSCaCO_3NP$ and Cur-$CSCaCO_3NP$ were examined by Transmission electron microscope (TEM), Field electron-surface electron microscope (FESEM), Fourier transform infrared rays (FT-IR), X-ray diffractometer (XRD), Zeta sizer and Brunauer-Emmett-teller (BET) for determination of size and shape, surface morphology, functional groups, purity and crystallinity, surface charge and polydispersity index (PDI), and pore size and surface area respectively.

2.6.1 *Determination of Nanosize and Shape using TEM*

The size and shape of $CSCaCO_3NP$ and Cur-$CSCaCO_3NP$ were determined using TEM (Hitachi H-7100, Japan). Both separate Samples (0.1 mg each) were suspended dropwise in 1 ml of acetone (45% alcohol) plus 2 ml of deionized water for 30 min ultra-sonication (Power Sonic 505, South Korea). The supernatant was added in dropwise to 200-mesh carbon coated copper grid (Sigma-Aldrich, USA), excess liquid was blotted out using filter paper and was dropped on the Whatman paper (Fisher Scientific, Malaysia) in a petri dish after which it was air dried at room temperature and preserved in a desiccator for 48 hrs before viewing. The TEM measurement was carried out at 150 k [22,35].

2.6.2 *Determination of Surface Morphology using FESEM*

 doi:10.20944/preprints201908.0254.v1

Cross-sectional surface morphology of $CSCaCO_3NP$ and Cur-$CSCaCO_3NP$ were determined using FE-SEM (JOEL 7600F, JEOL, Munchen, Germany). Thin layer of gold palladium coated with samples (5 × 5 mm) placed on adhesive stubs and viewed. The working voltage of FE-SEM was at 5.0 kV.

2.6.3 Chemical Spectroscopy using a Fourier Transform Infrared Rays (FT-IR)

Potential interactions between the chemical constituents to depict the functional groups of $CSCaCO_3NP$, Cur-$CSCaCO_3NP$ and free Curcumin were analyzed by FT-IR (Model 100 series, Perkin Elmer) at a range of 4000 cm^{-1} to 400 cm^{-1} with a resolution of 1 cm^{-1} and average scan of 64 times.

2.6.4 XRD-Powder Diffraction Determination

The purity and crystallinity of CSCaCO3NP, Cur-CSCaCO3NP and free curcumin were assessed using an X-ray powder diffractometer (Shimadzu XRD-600 powder diffractometer, Japan) equipped with CuK (A= 1.540562 nm) at 30.0 kV and 30 mA. The phase of each sample was determined based on diffraction angles of 5.0°-60° continuously at room temperature. The radiation source was scanned at the rate of 2.00 (deg/min).

2.6.5 Particle Size and Zeta Potential Analysis

The mean size diameter, PDI and surface charge (zeta potential) of $CSCaCO_3NP$ and Cur-$CSCaCO_3NP$ were measured with a Zeta-sizer Nano ZS, Malvern instrument (Malvern Version 7.02, Malvern Instruments Ltd. UK). About 0.1 mg of $CSCaCO_3NP$ and Cur-CSCaCO3NP were dissolved separately in 12 ml of pH 7.4 solution (normal physiological condition) and ultra-sonicated for approximately 30 minutes at room temperature prior to the analysis. The supernatant was loaded into a disposable cuvette using a syringe attached with 0.2 µL filter. The analysis was performed at 25 °C with dynamic light scattering detected at angle 90°. The uniformity of the size distribution was determined from the PDI. All the measurements were made at a constant solution in triplicates (n = 3) and the average values was taken to determine the zeta potential as earlier described [25,36].

2.6.6 Pore Size and Surface Area Determination using BET

The surface area to volume ratio analysis was done in accordance with previous studies with slight modifications [22,25]. The pore size and specific surface area of the $CSCaCO_3NP$ was determined using 3-flex surface characterization analyzer (The Brunauer-Emmett-teller Micrometrics, Instrument Corporation, version 1.02, USA) which was incorporated with nitrogen gas adsorption/desorption isotherm at 77.219 K using a total sample weight of 0.2065 g. Initially, the sample was outgassed at 90 °C for 60minutes using the equilibrium interval of 10 s and a sample density of 1.0 g/cm^3. Base on the adsorption and desorption isotherm at a relative pressure ($P/P0$) range of 0.009 to 0.13. The data obtained were analyzed using the BET and Barrett-Joyner-Halenda (BJH) models to determine the BJH mean pore size distribution, isotherm type, the total volume of pore size and BET specific surface area.

2.7 In Vitro Kinetic Release of Curcumin from $CSCaCO_3NP$

The *in vitro* release of curcumin from $CSCaCO_3NP$ was determined in simulated gastric pH 1.2 (high acidic medium), the normal physiological condition (pH 7.4) and pH 4.8 (less acidic medium) simulating the blood, oesophagus, intestine and cells microenvironments at ambient temperature (Table A1). The process was performed using a dialysis bag membrane method according to

 doi:10.20944/preprints201908.0254.v1

procedures described by previous literatures with slight modifications [24,37]. 10 mg of three (3) separate samples of Cur-CSCaCO$_3$NP in 1ml of deionized water and 10 mg of free curcumin in 1 ml (100 µL of ethanol and 900 µL of deionized water) were put in a dialysis bag which were suspended in a glass jar containing 100 ml of each previously mentioned pH solutions respectively. The free curcumin solution was suspended separately in simulated gastric pH 1.2 as blank control to serve for a comparison with Cur-CSCaCO$_3$NP. Afterward, a magnetic stirring bar was placed in each of the four solutions and placed on a digital magnetic stirring machine at 100 rpm. This was carried out at 37 °C with slow constant stirring. At regular time intervals (0, 0.5, 1, 4, 6, 8, 12, 24, 48, 72, 96, 120, 144 and 168) hrs, 1000 µl of each solution were pipetted into 96 well plate for absorbance measurements and were replaced with equivalent volumes of the resultant fresh pH solutions to keep the volume constant. Drug release concentrations were determined at specific intervals by measuring the absorbance at 430 nm using UV-vis spectrophotometer (PerkinElmer Lambda 35 Boston, MA, USA). The calculations were according to the standard curve prepaid in concentration gradients of free curcumin at the range of 0.5-2 mg/ml (Figure A1). The experiment was repeated in triplicates with the concentration of curcumin released in the various simulated mediums expressed as a percentage of the initial sample (Equation 3). The release kinetics of Cur-CSCaCO$_3$NP were studied using Korsmeyer-Peppas, Higuchi and zero order equation models and the data generated were plotted using regression analysis [38,39].

$$Curcumin\ released\ (\%) = \frac{\text{Concentration of curcumin released}}{\text{Initial total curcumin concentration}} X\ 100 \quad \ldots (3)$$

2.8 Data Analysis

The data obtained are expressed as mean ± standard error of mean (SEM). p value less < 0.05 was considered significant where applicable. Two-way ANOVA and linear regression analysis were employed. The data analysis was conducted using GraphPad prism (GraphPad Prism software, Inc, Version 6.01, San Diego, California, USA), OriginPro version 9.0 32Bit.Ink and SPSS version 25 softwares.

3. Results

3.1. Encapsulation Efficiency (EE) and Loading Capacity (LC)

Curcumin was successfully loaded onto CSCaCO$_3$NP with variations on the loading capacity and high efficient encapsulation. A clear summary of the loading capacity and encapsulation efficiency of CSCaCO$_3$NP to curcumin is shown in Table 2, with differences exhibited by CSCaCO$_3$NP on the loading capacity and encapsulation efficiency. Good encapsulation efficiency and loading capacity were observed in all the theoretical ratios. Although, equal ratios of CSCaCO$_3$NP to curcumin (Code 2 and 6) provided a high LC % and EE %, however, Code 4 with ratio of CSCaCO$_3$NP 1:3 curcumin (10 mg of CSCaCO$_3$NP and 30 mg of curcumin) as shown in Table 2, was chosen for subsequent analysis of this study. The EE was affected by the amount of curcumin with reference to the different ratios of the curcumin to nanoparticles used; hence, the total percentage entrapments were seen decreasing as the amounts of curcumin increases. Cur-CSCaCO$_3$NP was seen to be soluble after loading with the nanoparticle (Figure 1) although, the yellow coloration was still visible.

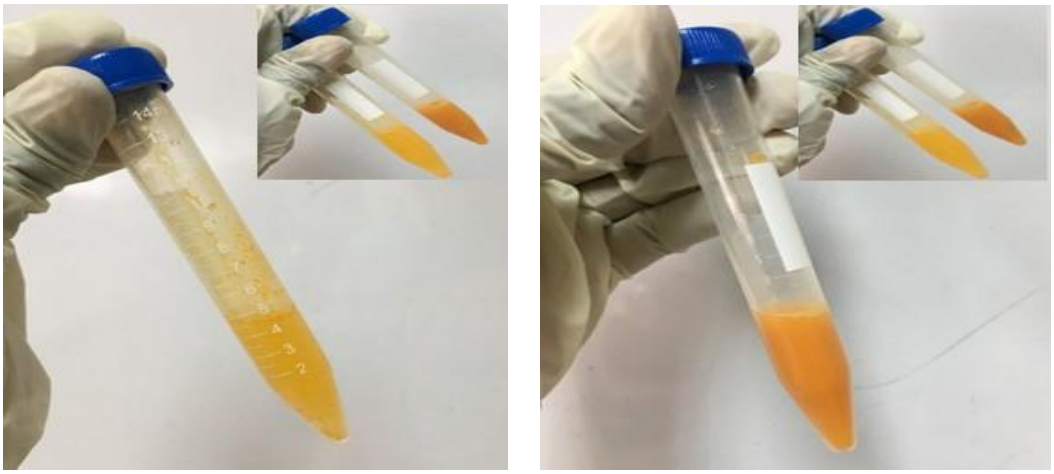

(a) **(b)**

Figure 1. Effect of $CSCaCO_3NP$ on the solubility nature of curcumin in aqueous solution (a) before loading with $CSCaCO_3NP$ (b) after loading with $CSCaCO_3NP$

Table 2. Effect of the Weight of Curcumin on $CSCaCO_3NP$ on the Loading Capacity and Encapsulation Efficiency.

CODE	$CSCaCO_3NP$ (mg)	CURCUMIN (mg)	DRUG FED (mg)	LC%	EE %	RATIO
1	20	30	17.90	89.49	59.66	2:3
2	20	20	12.60	62.99	62.99	1:1
3	20	10	9.35	46.76	93.52	2:1
4	**10**	**30**	**9.76**	**97.58**	**32.53**	**1:3**
5	10	20	7.20	71.97	35.98	1:2
6	10	10	9.90	99.03	99.03	1:1

3.2 TEM

Spherical shapes with porosity was observed on TEM (Figure 2a) with an average mean diameter of 21.38 ± 2.7 nm as seen in Figure 2(b). Also, spherical shaped nanoparticles were observed after loading (Cur-$CSCaCO_3NP$) as seen in Figure 3(a) with an average mean diameter of 45.32 ± 5.05 nm (Figure 3b). The Gaussian distribution of $CSCaCO_3NP$ and Cur-$CSCaCO_3NP$ revealed a uniform distribution of the nanoparticles (Table 3). Additionally, notable rough porous nature of $CSCaCO_3NP$ with some agglomerations were observed.

Preprints (www.preprints.org) | NOT PEER-REVIEWED | Posted: 25 August 2019 doi:10.20944/preprints201908.0254.v1

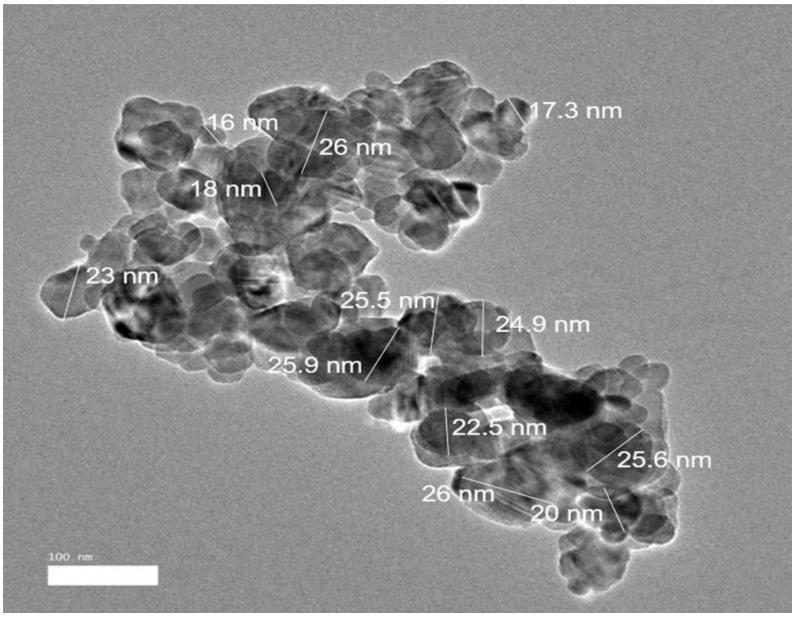

(a)

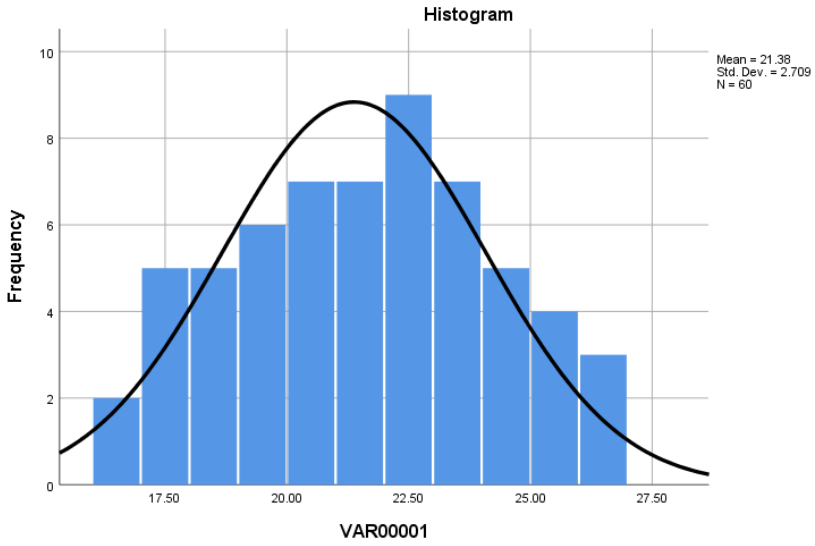

(b)

Figure 2. CSCaCO$_3$NP (a) TEM micrograph of spherical shaped CSCaCO$_3$NP (b) A histogram showing the average diameter size of 21.38 nm in distribution

Preprints (www.preprints.org) | NOT PEER-REVIEWED | Posted: 25 August 2019 doi:10.20944/preprints201908.0254.v1

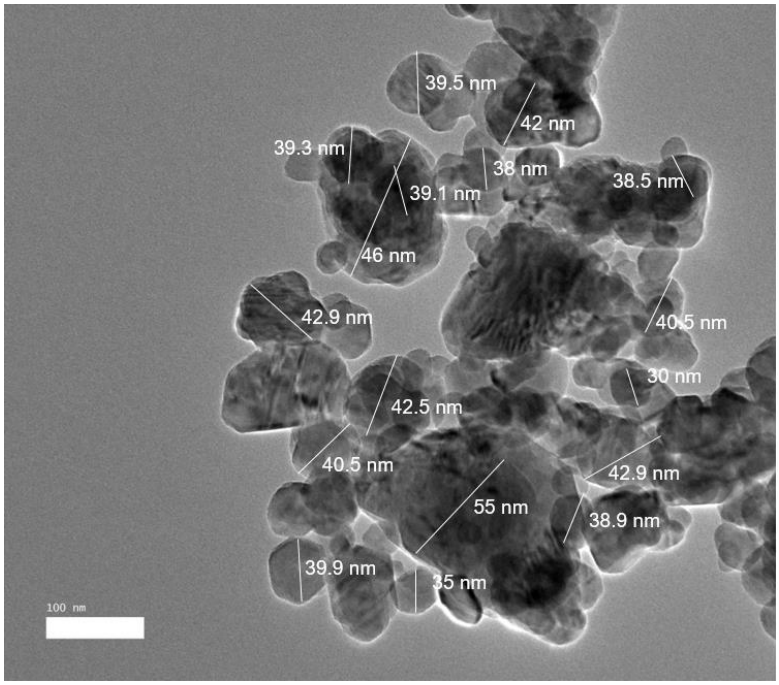

(a)

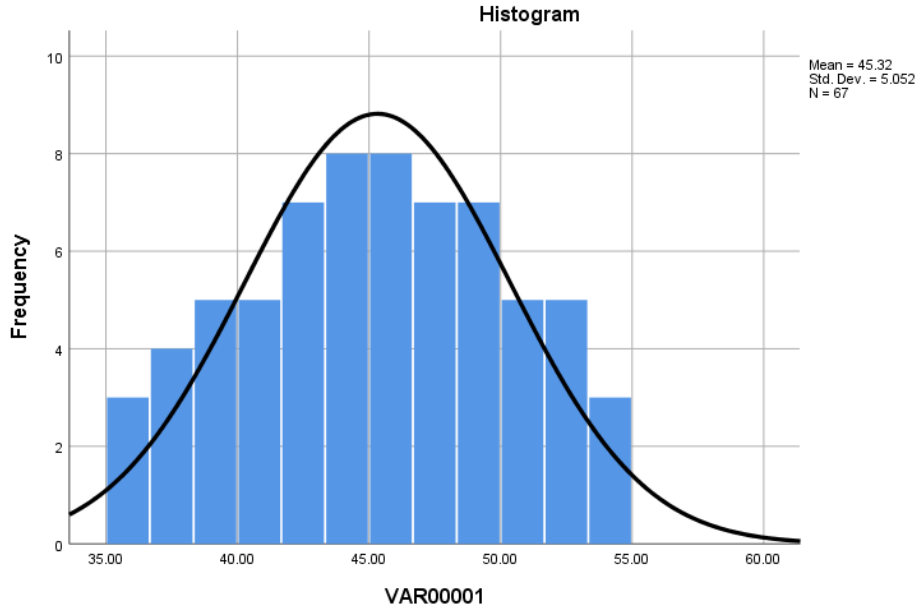

(b)

Figure 3. Cur-CSCaCO₃NP: (a) TEM micrograph of spherical shaped Cur-CSCaCO₃NP (b) A histogram showing average diameter size of 45.32 nm in distribution

Table 3. The average mean distribution of CSCaCO₃NP and Cur-CSCaCO₃NP

Nanoparticles	Diameter Size Mean ± SEM (nm)	Min. Value (nm)	Max. Value (nm)
CSCaCO₃NP	21.38 ± 3.7	16	26.20
Cur-CSCaCO₃NP	45.36 ± 5.05	35	55.00

 doi:10.20944/preprints201908.0254.v1

3.3 *FE-SEM*

The cross sectional view of the surface morphology of the synthesised $CSCaCO_3NP$ and Cur-$CSCaCO_3NP$ revealed numerous unidimensional spherical shaped nanoparticles which are fairly uniform in size and shapes with rough surfaces as shown in Figure 4 (a) and Figure 4 (b) respectively.

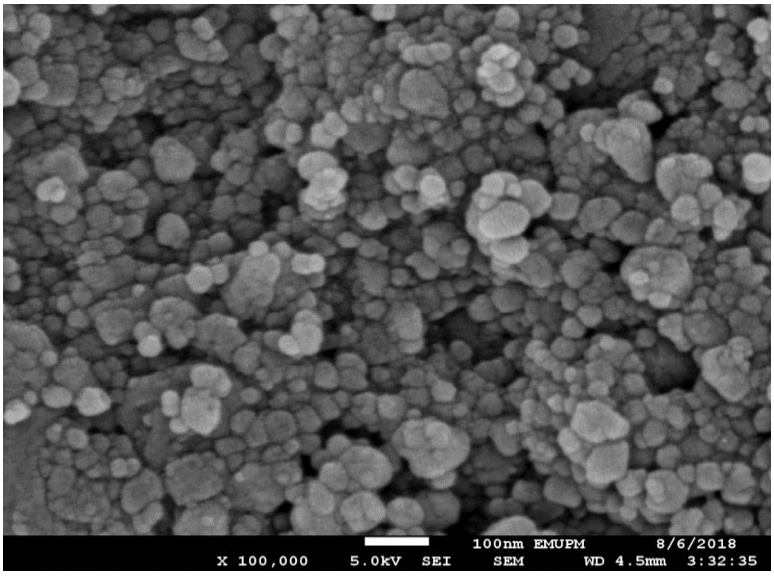

(a)

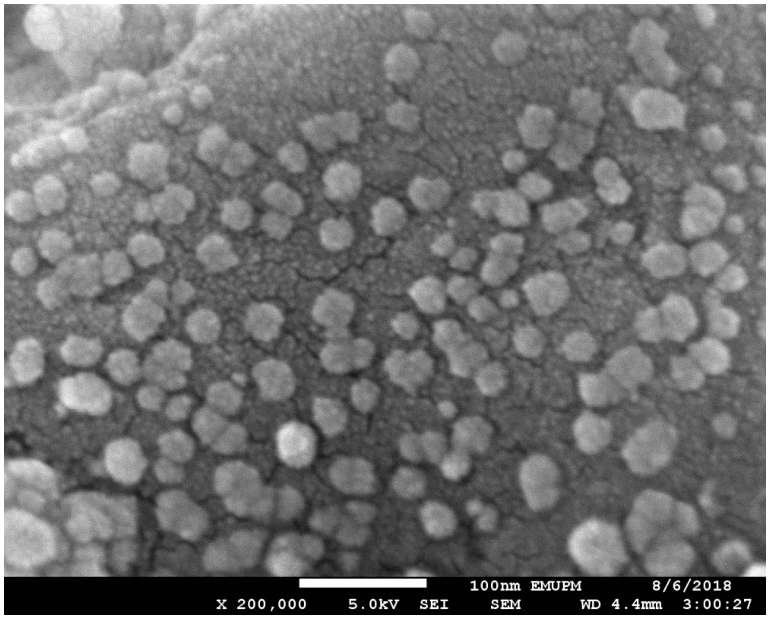

(b)

Figure 4. FE-SEM micrograph showing: (a) Spherical shaped $CSCaCO_3NP$ before loading (b) Spherical shaped Cur-$CSCaCO_3NP$ after loading

3.4 *Zeta Size, PDI and Charge Potential*

The zeta size of $CSCaCO_3NP$ revealed an average diameter of 50.09 ± 1.04 nm (range 48.44 – 55.00 nm) with a PDI of 0.17 and a low negative charge potential of -18.7 mV. An increase in size, PDI

Preprints (www.preprints.org) | NOT PEER-REVIEWED | Posted: 25 August 2019 doi:10.20944/preprints201908.0254.v1

and surface charge were seen in Cur-CSCaCO$_3$NP which were 140.06 ± 1.01 nm (range 137.2 - 144.1 nm), 0.25 and -29.4 mV respectively as shown in Table 4 and Figure 5 & 6.

Table 4. The Average Size, PDI and Charge Potential of CSCaCO$_3$NP and Cur-CSCaCO$_3$NP

	Zeta size		Zeta Potential
Nanoparticle	**(nm)**	**PDI**	**(mV)**
CSCaCO$_3$NP	50.09 ± 1.04	0.17	-18.7
Cur-CSCaCO$_3$NP	140.06 ± 1.01	0.25	-29.4

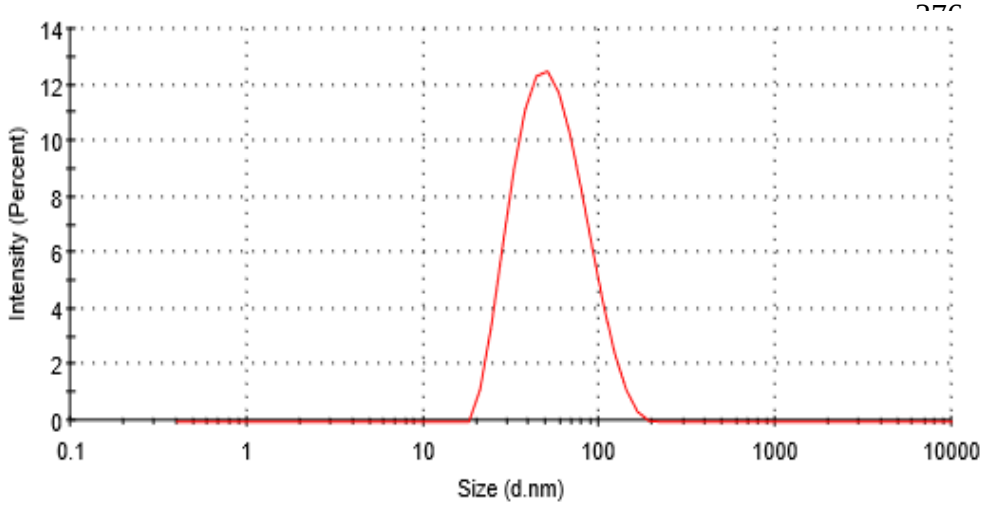

(a)

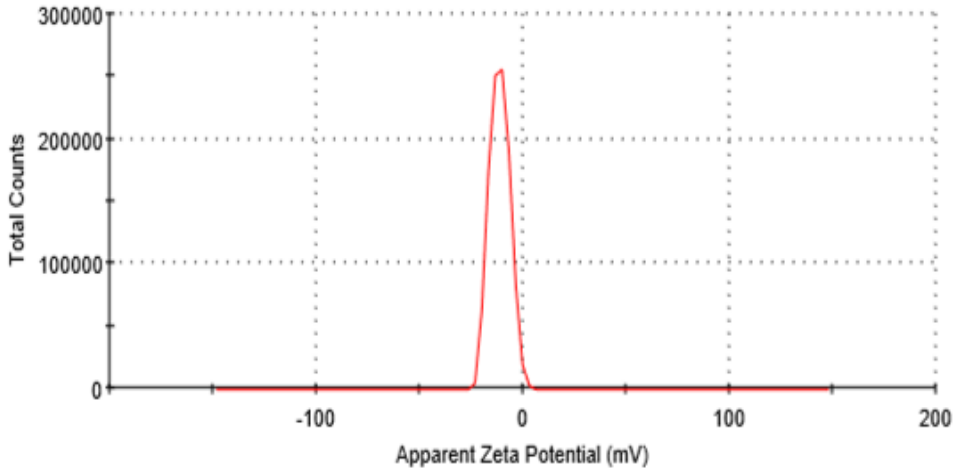

(b)

Figure 5. A graphical representation of CSCaCO$_3$NP showing: (a) An average mean diameter size of 50.09 ± 1.04 nm (b) Surface charge of -18.7 mV

 doi:10.20944/preprints201908.0254.v1

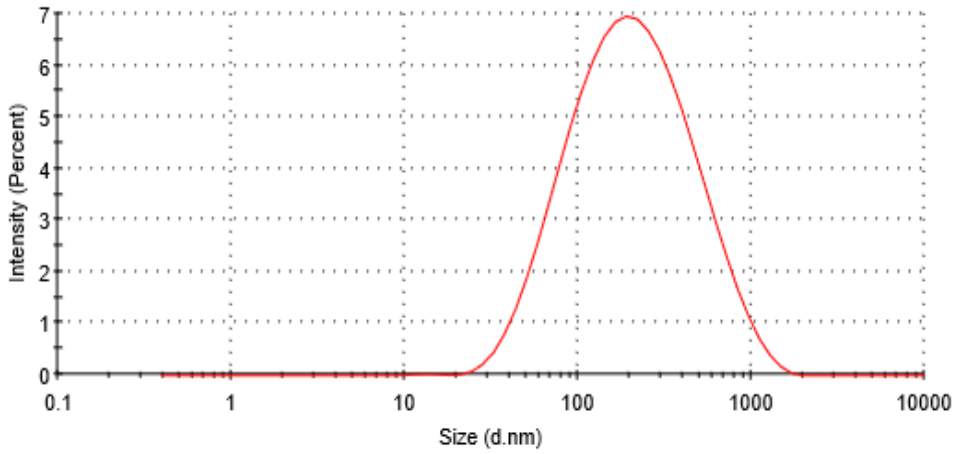

(a)

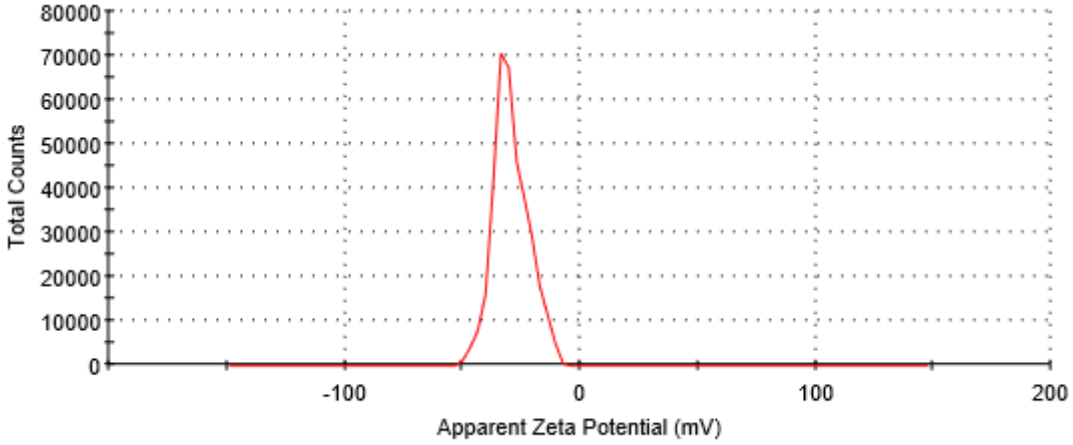

(b)

Figure 6. A graphical representation of Cur-CSCaCO$_3$NP showing: (a) An average mean diameter size of 140.06 ± 1.01 nm (b) Surface charge of -29.4 mV.

3.5 FT-IR

The characteristics bands of CSCaCO$_3$NP, Cur-CSCaCO$_3$NP and free curcumin were demonstrated by the absorption peaks spectra from the FT-IR spectroscopy. The spectral absorption peaks of CSCaCO$_3$NP were seen at 1786.08 cm^{-1}, 1446.61 cm^{-1}, 1082.07 cm^{-1}, 854.47 cm^{-1}, 713.66 cm^{-1}, and 462.92 cm^{-1} respectively indicating the presence of CO_3^{2-} carbonate ion on both CSCaCO$_3$NP and Cur-CSCaCO$_3$NP. The strong peaks of the three products indicated similar wavelengths, thus purity of the nanocarrier has not been altered by the preparation method. This confirmed a successful loading of the curcumin and strong conjugation between the two compounds (Figure 7).

Preprints (www.preprints.org) | NOT PEER-REVIEWED | Posted: 25 August 2019 doi:10.20944/preprints201908.0254.v1

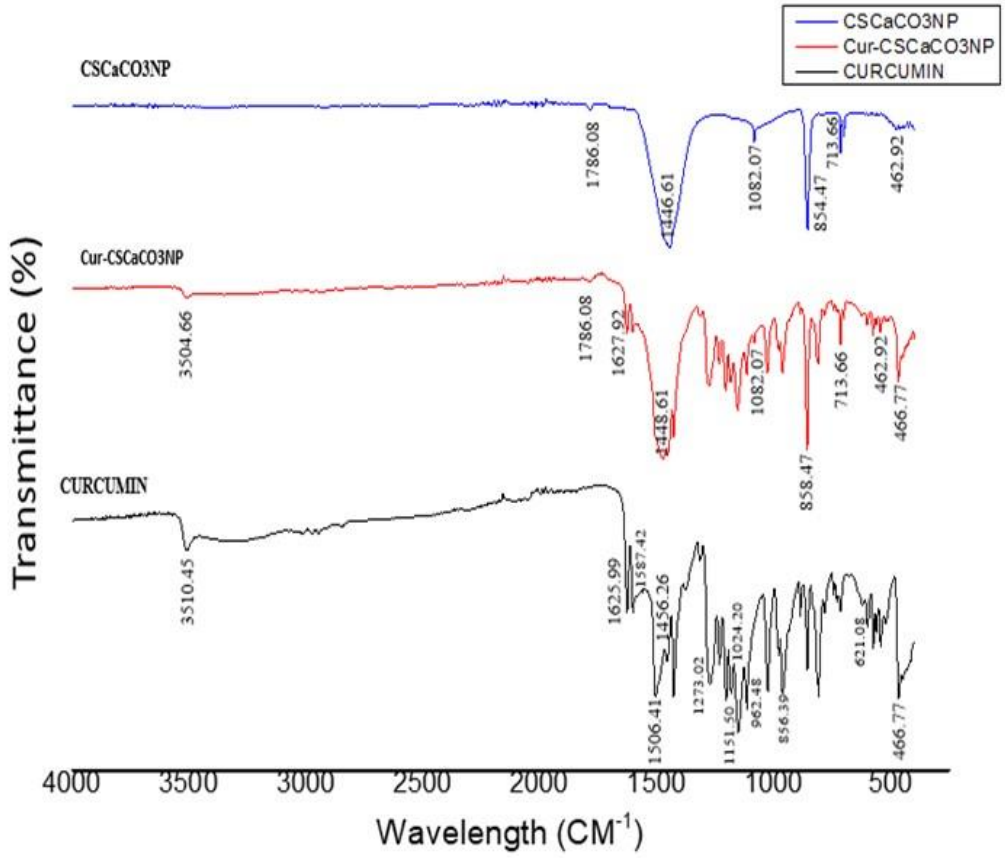

Figure 7. A graphical representation of an elementary analysis showing the functional group endings of $CaCO_3$NP, Cur-CS$CaCO_3$NP and curcumin.

3.6 XRD

Crystallinity and purity nature of CS$CaCO_3$NP, Cur-CS$CaCO_3$NP and free curcumin were analyzed using XRD, which is a strong analytical tool, used for assessing the purity nature and crystalline phases of sample particles. The similarities in the absorption peaks of CSCaCO3NP and Cur-CS$CaCO_3$NP at 2 theta of 26.17°, 28.22°, 33.5° and 45.81° demonstrated the unchanged nature of crystalline phase of CS$CaCO_3$NP after loading with curcumin. The free curcumin demonstrated some sharp peaks at a diffraction angle of 8° - 28.92° indicating a high crystalline nature (Figure 8).

Preprints (www.preprints.org) | NOT PEER-REVIEWED | Posted: 25 August 2019 doi:10.20944/preprints201908.0254.v1

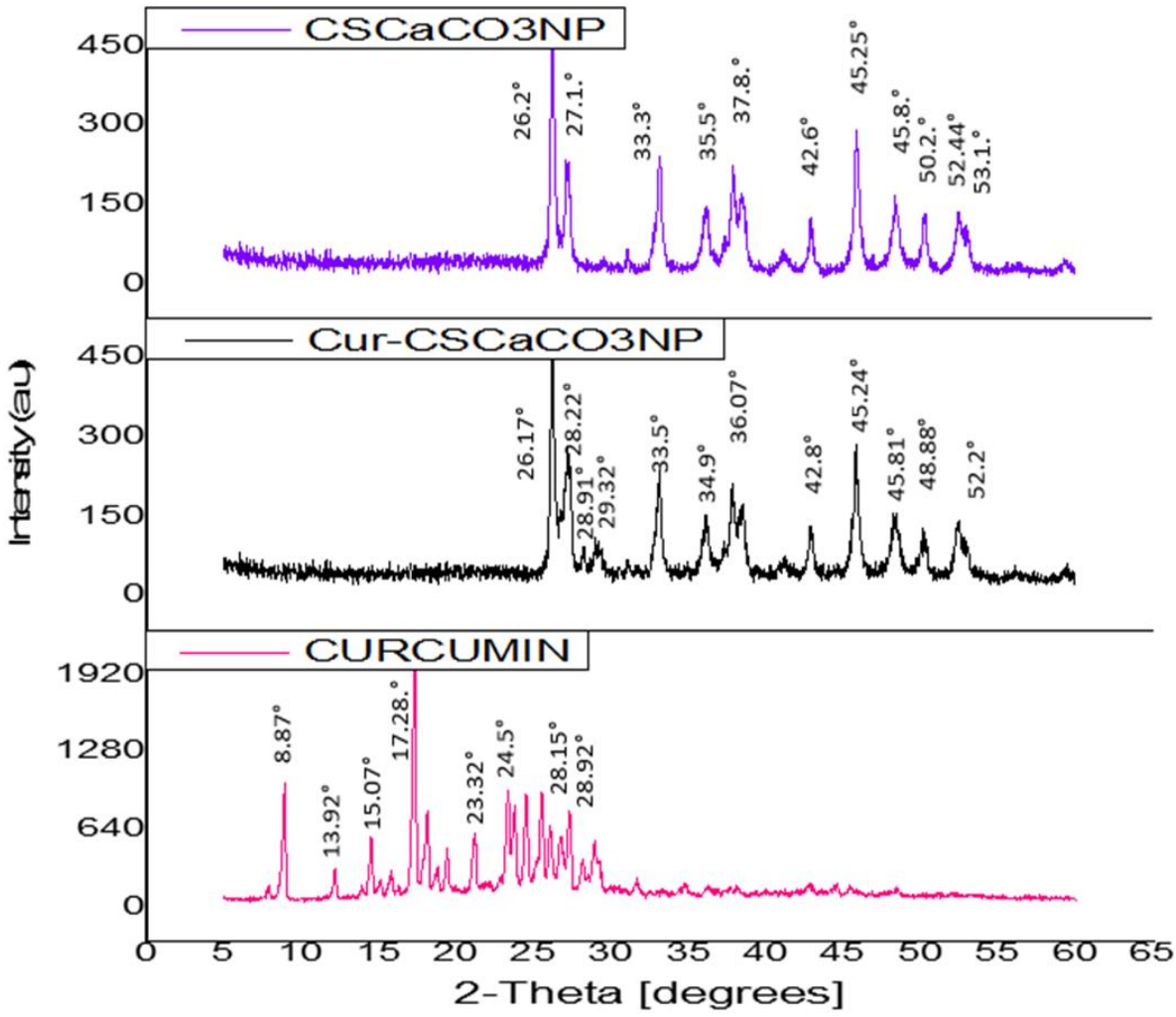

Figure 8. The XRD pattern (X-Ray Diffraction spectra) of $CSCaCO_3NP$, Cur-$CSCaCO_3NP$ and curcumin

3.7 Brunauer-Emmett-Teller isotherm (BET)

The synthesized $CSCaCO_3NP$ revealed an adsorption/desorption isotherm graph of type III mesoporous with hysteresis loop showing the presence of multiple layers with a sharp curve at a relative pressure of 0.009 to 0.13 (Figure 9). The BJH mean pore size diameter and BET specific surface area are 3.35 nm and 14.4806 ± 0.110 m^2/g respectively (Table 5).

Table 5. The BJH desorption mean pore size and BET specific surface area of $CSCaCO_3NP$.

Sample	BJH mean pore size diameter (nm)	Specific Surface area BET (m^2/g)	Total volume of pores at P/Po at 0.9889 (cm^3/g)
$CSCaCO_3NP$	3.35	14.4806 ± 0.110	0.1211

Preprints (www.preprints.org) | NOT PEER-REVIEWED | Posted: 25 August 2019 doi:10.20944/preprints201908.0254.v1

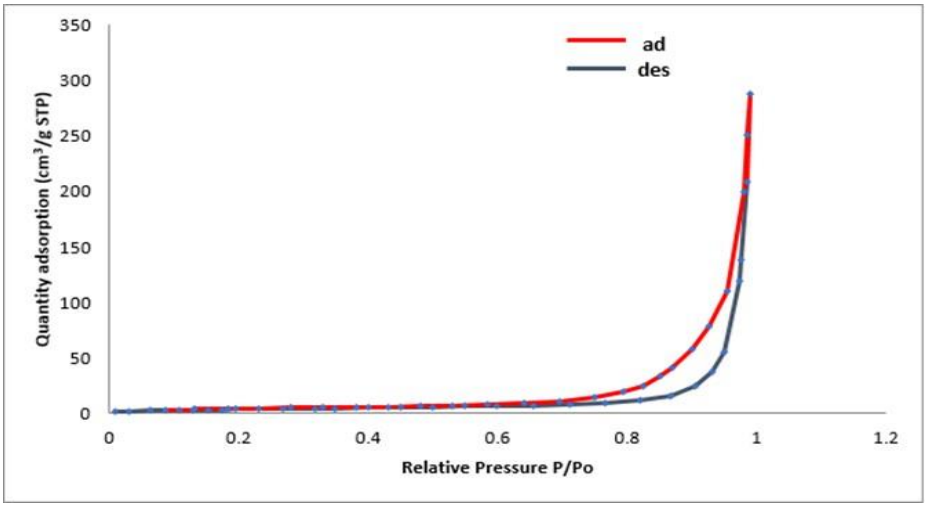

Figure 9. Brunauer-Emmett-Teller Isotherm Graph of CSCaCO$_3$NP

2.8. In Vitro Release Profile Studies

The kinetic release profile of curcumin from CSCaCO$_3$NP is demonstrated in Figure 10. Free curcumin was used as a positive control in the kinetic assay studies. Cur-CSCaCO$_3$NP demonstrated a slow sustained kinetic release pattern of curcumin from the core shell of CSCaCO$_3$NP as compared to the release pattern of free curcumin from the dialysis bag. At the first phase, there was an initial slow release phase of curcumin from the core of CSCaCO$_3$NP in pH 4.8 (2%), pH 1.2 (3%) and pH 7.4 (5%) when compared to the rapid release phase of free curcumin from the membrane bag in pH 1.2 (20%). However, a steady increasing release phase was observed for Cur-CSCaCO$_3$NP in all the pH environments with a sudden outburst release patterns amounting to the following percentages: pH 4.8 (30%), pH 1.2 (24%) and pH 7.4 (40%) when compared to the fast continuous release of free curcumin in pH 1.2 (70%) at 24 hrs. Finally, the plateau phase lasted for 168 hrs accumulating to the following percentages release of curcumin from Cur-CaCO$_3$NP: pH 4.8 (64%), pH 1.2 (56%) and pH 7.4 (78%) when compared to the final release phase of free curcumin in pH 1.2 (94%). The data generated were fitted into three different kinetic equations and base on the co-efficient of determination (R^2) using linear regression analysis. The Higuchi kinetic equation model [pH 7.4 (R^2 = 0.9472) and pH 1.2 (R^2 = 0.9632)] is the best fit when compared to the Korsmeyer-Peppas [pH 7.4 (R^2 = 0.9076) and pH 1.2 (R^2 = 0.9615)] and Zero order [pH 7.4 (R^2 = 0.8067) and pH 1.2 (R^2 = 0.8513)] kinetic models as shown Figure 11 and 12.

 doi:10.20944/preprints201908.0254.v1

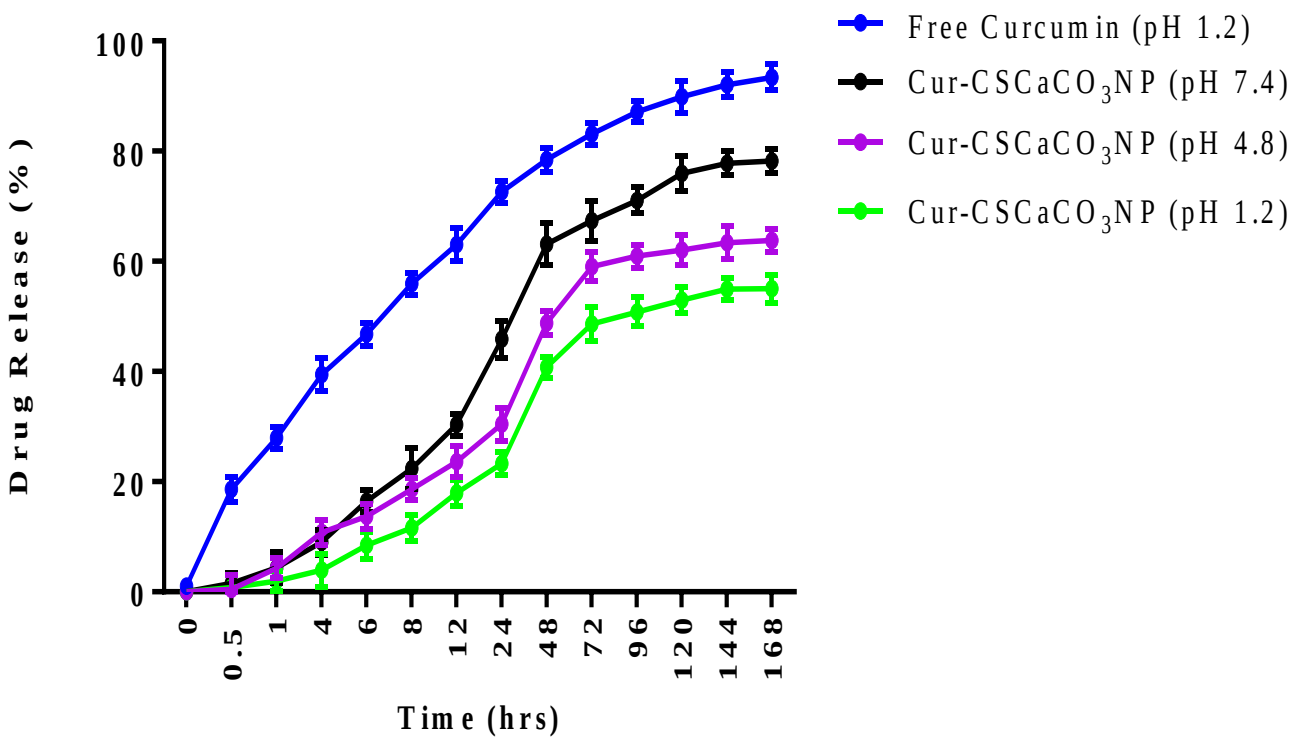

Figure 10. A cumulative release curves of free curcumin and Cur-CSCaCO3NP in different pH medium at different time points showing variations on the release of curcumin *in vitro*. Triplicate data and values are expressed in mean ± SEM (n=3)

Preprints (www.preprints.org) | NOT PEER-REVIEWED | Posted: 25 August 2019 doi:10.20944/preprints201908.0254.v1

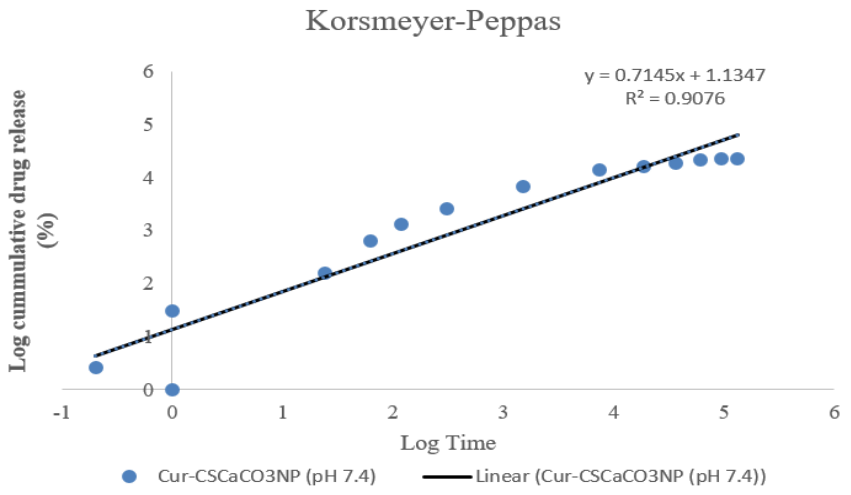

(a)

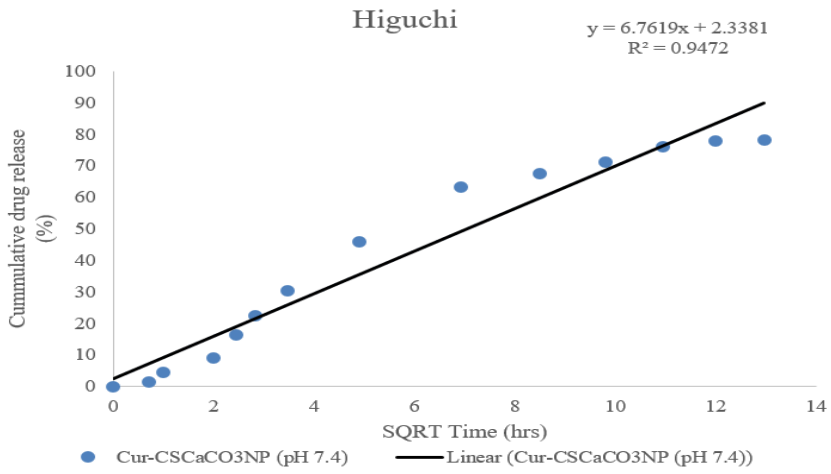

(b)

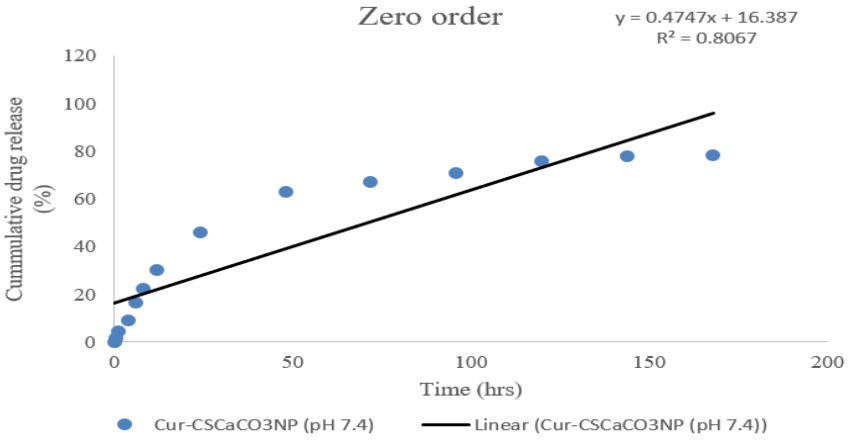

(c)

Figure 11. Fitting experimental data of Cur-CSCaCO$_3$NP release in pH 7.4 medium (a) Korsmeyer-peppas release model (b) Higuchi release model (c) Zero order release model.

 doi:10.20944/preprints201908.0254.v1

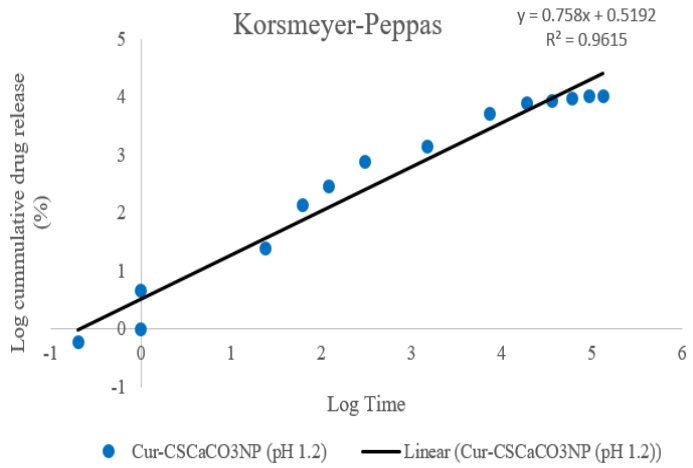

(a)

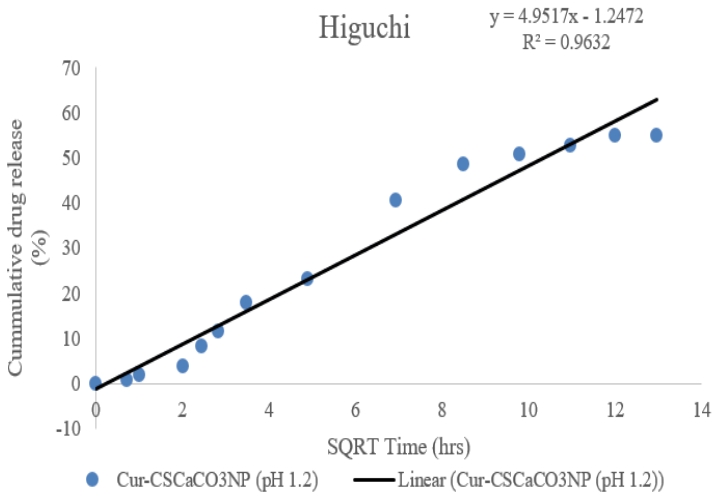

(b)

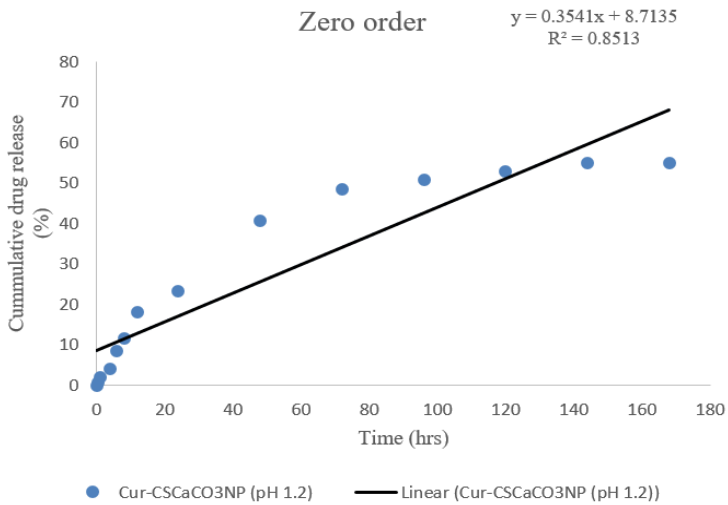

(c)

Figure 12. Fitting experimental data of Cur-CSCaCO$_3$NP release in pH 1.2 medium (a) Korsmeyer-peppas release model (b) Higuchi release model (c) Zero order release model.

 doi:10.20944/preprints201908.0254.v1

4. Discussion

Adopting an improved method of top-down development of CSCaCO3NP by previous literatures, while improving other parameters therein (time, drying, temperature and stirring speed) provided a better smaller size and larger surface area for the nanoparticles used in this study. The high loading content and encapsulation efficiency of CSCaCO3NP for curcumin were further supported by the large surface area and pore size volume obtained. In the current study, entrapment of curcumin onto the newly synthesized nanocarrier greatly improved curcumin's solubility. Cur-CSCaCO3NP demonstrated a sustained kinetic release with a better slow release pattern observed at pH 1.2 when compared to the sustained release profile observed at pH 7.4 and free curcumin at pH 1.2. These observations showed that large amount of curcumin was encapsulated into the matrix of CSCaCO3NP, resulting in pH and time dependent release pattern associated with strong effect of the properties of curcumin. In addition, Higuchi equation model best described the nature of CSCaCO3NP release.

Although curcumin has poor solubility in aqueous medium, the loading of curcumin on the new synthesized nanocarrier in the present study has increased its solubility. This is in agreements with earlier studies that reported enhanced curcumin solubility when load onto nanocarriers [29,32,40]. Additionally, the higher encapsulation efficiency and loading capacity observed in all the different theoretical ratios of curcumin to nanoparticles regardless of the differences in the ratio amounts, is suggestive of a strong interactions of the curcumin molecules with CSCaCO3NP. This is because the negatively charged CSCaCO3NP highly attracted the positively charged curcumin, therefore, electrostatic attractions occurred [41]. The ratio chosen for the subsequent analysis in this study was due the small amount of CSCaCO3NP used in encapsulating high amount of curcumin. Hence, provided a better optimum percentage suitable for the entrapment of curcumin in the coreshell of the nanoparticles. This showed that few amount of curcumin was lost during loading process, thus, more curcumin molecules could interact with molecules of the nanoparticles resulting to a fair amount of curcumin being encapsulated [8,23–25]. The findings of the present study revealed less curcumin wastage and minimal usage of CSCaCO3NP. Interestingly, CSCaCO3NP has been reported to exhibit nanopores feature which gives room for high loading capacity by means of capillary force interactions [24,41,42]. It can be deduced that the EE% decreases with a corresponding increase in the amount of curcumin while LC% increases with a corresponding decrease of curcumin in this study.

In the present study, a small average mean diameter of CSCaCO3NP and Cur-CSCaCO3NP were produced although, with presence of some agglomerations which is peculiar to CaCO3NP due to its hygroscopic nature, this is in conformism with earlier studies where similar occurrences were reported[43–45]. The small average mean diameter obtained could increase the oral bioavailability of curcumin since it is well documented that a particle size reduction could increase drug efficacy and promote efficient interfacial interaction with the cell membrane as a result of endocytosis of small sized particles compared to larger ones [46]. However, particle size less than 5 nm are likely to be eliminated by the kidney before reaching their target site while larger particle size above 200 nm easily gets sequestered by the liver and spleen at the reticuloendothelial system [47]. The size diameter obtained for CSCaCO3NP in this study falls within the effective range that could be administered for therapeutic purposes. In addition, nanoparticle of size < 200 nm showed improved long period of circulation in the body and as well experiences decrease in the hepatic filtrations [48].

 doi:10.20944/preprints201908.0254.v1

Although, this study recorded a double increase in the size of the nanoparticle after loading with curcumin, which is as a result of the amounts ratios of the two compound used during the loading process resulting to possible higher entrapments of the smaller curcumin molecules at the core shell and surface of the nanoparticles leading to the increase in size. This increase in size of the nanoparticles upon loading has been reported in the previous literatures [22,25,48]. The sizes obtained for Cur-CSCaCO$_3$NP falls within the acceptable range for effective oral administration since a better drug release control and cell infiltration nature has so far been demonstrated by nanoparticles below 100 nm [30]. Interestingly, porosity was clearly observed on CSCaCO$_3$NP which is likely a credit to high loading and encapsulation efficiency recorded, which were all in agreements with the findings of other studies after subjecting the nanoparticle to TEM machine for diameter size analysis [22,25,49,50].

FE-SEM revealed that the surface morphology of CSCaCO$_3$NP before and after loading with curcumin to be uniform and spherically shaped. Contrary to the present findings, Islam et al. [3], Kamba et al. [51] and Hoque et al. [52] reported a rod-like shape for CSCaCO$_3$NP. However, variation in the size and shape of nanomaterials may be influenced by the source of the biomaterial used and the method employed during the synthesis [20,22,25]. Spherically shaped biogenic nanoparticles were reported to possess large surface area for interactions with biological systems thereby making them an excellent nanocarriers [22,25]. Spherical nanoparticles were seen 500 % efficiently taken up by cells compared to the rod-shaped nanoparticles due to the prolonged membrane engulfment time needed for the lengthy shaped nanoparticles [53]. Thus, suggesting that the spherical shape obtained for CSCaCO$_3$NP and Cur-CSCaCO$_3$NP in this study is suitable for the delivery of therapeutic agents. However, minute aggregations were observed before loading, this is due to the method adopted for the preparation of the sample for FE-SEM analysis, which allowed fast absorption of moisture from the environment [50]. The absence of aggregations after loading could be due to curcumin chemical properties being hydrophobic which could slightly affect the hydrophilic nature of the nanoparticle and thus, prevent it from absorbing moisture from the environment [49].

The inherent polydispersity of nanoparticles influences any predictable contact behavior of the nanoparticles with cells [9,49]. While neutral functional groups are reported to excellently prevent the invading of unwanted nanomaterial into the biological system, majority of the charged functional groups of nanoparticles greatly affects cellular interactions, thus serving as excellent driving force for active nanoparticles to interact with cells [54]. The zeta sizer results in this study, depicted that the net charge of the formulations were negative which provided a high affinity for curcumin during loading, as such the charge potential increased after loading with curcumin which indicated a stability and a strong loading efficiency, this is in agreement with the work of Rejinold et al. [31], who reported an increase in charge potential of fibrinogen after loading with curcumin. The high negative charge obtained for both CSCaCO$_3$NP and Cur-CSCaCO$_3$NP indicates stability of the compound, which is attributable to the strong electro-static repulsion between the nanoparticles. Similar findings were reported in previous literatures [9,51]. The low PDI obtained indicated a good uniformity of size distribution of the nanoparticles. Increase in the hydrodynamic diameter seen in this study after loading was perhaps as a result of the drug fed onto the core shell of the nanoparticles as well as the surface attachment of the curcumin molecules to the nanoparticles which led to an increase in the

 doi:10.20944/preprints201908.0254.v1

size of the nanoparticles. Similar, findings were reported in previous studies [29,55]. Further, the difference in the particle size observed with the nanocarrier on TEM and FESEM compared to the size obtained on hydrodynamic analyzer were probably due to the water absorbed by the particles suspended in water, while absolute dried samples were used on the electron microscopes as described by Lozano-Pérez et al. [56] and Montalbán et al. [29]. In addition, the hydrophobic and electrostatic nature of interaction between CSCaCO$_3$NP and curcumin could result to high strong bonding at the core and surface attachment of the nanoparticles. However, these variations in size between electron microscopic measurement and hydrodynamic analyzer could be attributable to the presence of strong electrostatic repulsion between the nanoparticles in hydrodynamic motion during measurement [45]. Another possible reason could be due to the influence of agglomeration tendency on the size distribution of the particles in motion due to the increase seen in the PDI of particle after loading [57]. Similarly, previous findings documented size variations when different techniques were adopted [29,36,45]. Thus, the TEM and FESEM measure the diameter of the particle in real time with simple principle of electron beam with single particle measured while hydrodynamic analyzer uses the principles of both hydrodynamic and light. High positive or negative values of zeta potential above ± 30mV of a nanoparticles, indicates excellent stability and avert particles agglomerations due to electrostatic stabilization [22,24]. Perhaps, this explained the aggregation observed in this study, which possibly led to the increase in size of the nanoparticles.

Encapsulation of curcumin by CSCaCO$_3$ aragonite nanoparticles in this study was proven by the FT-IR analysis. The characteristic peaks shown by CSCaCO$_3$NP are within the ranges of the aragonite spectra peaks. The peaks were described to be the peaks of CO_3^{2-} that corresponds to the v1-v4 vibrations with little structural changes and this is attributable to the shift of the carbonate vibrations in the milieu of oxygen atoms and the modification in the electrostatic valence force that exists in Ca-O bond [58,59]. In addition, the sharp peak at 1082.07 cm^{-1} signifies characteristics aragonite phase of CaCO$_3$ spectrum whose ions were vague in the infrared region as reported in the preceding studies [20,22]. The band at 1446.61 cm^{-1} indicates C=C stretching frequency and 854.47 cm^{-1} and 713.66 cm^{-1} specifically shows the presence of carbonate (CO_3^{2-}). These findings were similar with previous documented findings [20,22,25,58]. Less observable characteristics reduction on the band was seen in the stretching frequency of Cur-CSCaCO$_3$NP, which depicted slight negligible shifts in the peak of the curcumin spectrum, which is due to the bond formation between the two compounds after curcumin encapsulation. Meanwhile, the absence of any great shift of the CSCaCO$_3$NP on Cur-CSCaCO$_3$NP spectrum suggested that the aragonite nanoparticles phase is intact and unaltered during the drug loading process. These were all in accordance with the work of Fu et al. [23], who reported negligible shifts of aragonite band when loaded with doxorubicin. Thus, further explains the wavelength shift from higher to lower region of the frequency as earlier suggested by Rejinold et al. [31]. In addition, the presence of curcumin-typical peaks as shown on the loaded nanoparticles revealed an effective loading of curcumin onto the aragonite nanoparticles. The out of plane bending and symmetric stretching corresponds to different functional groups. The spectra peak of curcumin at 1627.92 cm^{-1} and 1427.32 cm^{-1} depicted C=C stretching, 1456.26 cm^{-1} represents the C=H which is as a result of olefinic bending vibration of the benzene ring, the absorption at peak 1151.50 cm^{-1} indicated a C-H stretching and the peak spectra at 1024.20 cm^{-1} may be due to the C-N stretch. The peak at 1506.41 cm^{-1} is as a result of the functional group of benzene ring with a bond of

C-O-C. However the strong most important ring of benzene ring at 1506.41cm^{-1} present in the free curcumin peaks is completely absent on the Cur-CSCaCO$_3$NP spectra indicating that free curcumin was loaded successfully onto CSCaCO$_3$NP. These results corresponds with previous findings on a co-encapsulation of curcumin and doxorubicin in poly(butyl cyanoacrylate nanoparticles) and chitosan [59], an achievable loading of curcumin onto polymeric nanoparticles [36], and nanocurcumin physicochemical fabrication [60]. Further, some important shifts are confirmed on the spectra of Cur-CSCaCO$_3$NP like the shift peak from 1600.92 cm^{-1} to 1602.85 cm^{-1} and a shift of 1427.32 cm^{-1} to 1429.25 cm^{-1}. The peaks at 1273.02 cm^{-1} and 856.39 cm^{-1} for the vibration of C-O in –C-OCH3 of phenyl ring was shifted to 1274.95 cm^{-1} and 858.47 cm^{-1} respectively. Thus, all in accordance with the result of Rachmawati et al. [61]. All the aforementioned strong peaks of curcumin concurs with those described in the previous literatures [29,36].

In the present study, the XRD pattern of the strong sharp peaks of free curcumin appeared to be absent on Cur-CSCaCO$_3$NP phase which suggested that the free curcumin was strongly entrapped and encapsulated at the nanocore of CSCaCO$_3$NP. Further, the absence of the sharp endothermic peaks of curcumin at 8°-23.5° regions of Cur-CSCaCO$_3$NP phase, strongly suggests stability, purity and solubility of the loaded nanoparticles since successful incorporation of curcumin at CSCaCO$_3$NP matrix was confirmed. These findings agreed with previous findings who explained the absence or negligence of any changes on the crystallinity phase of the loaded nanoparticles compared with the blank CSCaCO$_3$NP [8,22,24]. In addition, Karri et al. [62], reported absence of the strong peaks of curcumin that led to a change of crystallinity nature of curcumin to amorphous state after conjugation with chitosan nanoparticles. In this study, CSCaCO$_3$NP crystalline peaks was maintained after loading with free curcumin which promoted sustained release of curcumin from the loaded nanoparticles. These were in accordance with the work of Kamba et al. [51] and Hammadi et al. [25], who reported the prominent peaks of CSCaCO$_3$NP at 2 theta 26.5^o, 27^o and 33.3^o respectively, and Wang et al. [63] who documented the sharp peaks of free curcumin within the range of 10^o-30^o. Despite the absence of majority of the signal sharp peaks seen on the peaks of Cur-CSCaCO$_3$NP in this study, few peaks of curcumin were observed after loading. This confirmed the statement earlier that the entrapment of curcumin was done majorly at the core shell of the nanoparticles and few surface attachments.

In the current study, *in vitro* release assessment of curcumin at different pH was carried out to ensure an ultimate consistency for the steady release of curcumin when passing through the GIT to the other parts of the body when administered orally. The overall phases of curcumin release from CSCaCO$_3$NP indicated high stability of the system in all the different pH used indicating that curcumin was well retained onto the core shell of the nanoparticles [8]. Jain and Jain [2], described the final slow and steady release rate to be attributed to proper localization and entrapment of drugs at the inner core of the nanoparticles. However, in this study, the initial release observed after 30 mins in all the pH medium could be as a result of the excessive attachments of curcumin on the large surface area of the nanoparticle and those residues stacked at the edge of the membrane bag when tying. Thus, promotes the initial dissolution of the weakly bound curcumin molecules. This is in accordance with previous literature [64]. The high release pattern of free curcumin in acidic pH 1.2 from the initial stage to final is due to the absence of the carrier medium as reported by Chen et al.

 doi:10.20944/preprints201908.0254.v1

[65]. Thus, a direct contact of curcumin with acidic environment could lead to a fast release in the absence of a carrier medium. Perhaps, this would explain why orally ingested curcumin suffers fast digestion and rapid metabolism in the body as documented earlier [9,45]. In contrast, the slow and steady release of curcumin from CSCaCO$_3$NP at pH 1.2 means that curcumin loaded at the core shell of the nanocarrier could hardly be released in the gastric medium and so can easily bypass the fast digestion at the GIT with the help of the nanocarrier. This agreed with the reports of previous literatures [9,60,65]. Thus, CSCaCO$_3$NP could not be rapidly digested at the GIT by digestive enzyme but would rather be slowly degraded by enzymes released by the bacterial flora present at the intestine. This is in consistent with previous report [50], which revealed the optimum retention of $CaCO_3$ nanomaterials derived from egg shells at pH 1.2 when compared to the rapid degradation and fast release at pH 7.4. Thus, concluded that particles could be retained at the stomach then transit to the intestine for proper final release and absorption. In addition, Udompornmongkol and Chiang [36], reported only 2% release pattern of curcumin from polymeric nanoparticle at pH 1.2 compared to 80% release at pH 4.5. Further, the influence of the nature of the loaded drug cannot be left out during release mechanism, hence curcumin undergoes rapid degradation in both neutral and basic pH environment compared to acidic pH [65]. In addition, this release behaviour is consistent with Shao et al. [66]'s experimental results relating to ganoderma lucidum polysaccharide's release. The author observed a slow release at pH 1.7 as compared to the release at pH 7.4, thus went further to explain the possible ionization of carboxylic group at higher pH resulting to an increased in the electrostatic repulsion, which causes the polymer to loose.

Noteworthy, a notable high cumulative percentage of drug release from CSCaCO$_3$NP was observed in pH 4.8 than in pH 7.4 as reported by other scientists [23,25,42] thus, contrary to the current findings. Although, the aforementioned authors did not assess the release pattern in pH 1.2, which is a stronger acidic medium than the pH medium they used (pH 4.8) vice versa, failed to provide the knowledge on the fate of CSCaCO$_3$NP in strong acidic medium irrespective of the different candidate drug used. In this study, the high percentage release of curcumin at pH 7.4 observed when compared to the percentage release at pH 1.2 and pH 4.8 was due to the maximum sustained release of curcumin. Therefore, the release of the loaded curcumin at pH 1.2 indicated a high stability of Cur-CSCaCO$_3$NP, thus curcumin could be protected from stomach acidic content when orally administered. Further, apart from the protective effect of the nanocarrier for curcumin, the stability of curcumin was reported at low pH conditions which is attributable to its conjugated diene structure, likewise the instability of curcumin in neutral to basic medium is based on the removal of its proton from the phenolic group leading to its structural destruction [67]. This release pattern seen in this study is in accordance with the work of Render et al. [50] and Rejinold et al. [31]. Based on the sustained release pattern in strong acidic medium observed, conclusion can be deduced that the therapeutic efficacy of orally administered curcumin may be improved by encapsulation with CSCaCO$_3$NP since therapeutic efficacy of every encapsulated drug is directly proportional to the quantity of the drug released from the carrier system [68]. Further, there is a high tendency for efficient uptake of Cur-CSCaCO$_3$NP by the cells at the upper GIT before reaching the GIT proper to prevent possible contact with the gastric content, which may aid fast degradation and prolong circulation of the soluble curcumin in the blood, which will in turn improve its bioavailability.

 doi:10.20944/preprints201908.0254.v1

In the present study, the results of the kinetic models depicted the nature of the overall release of curcumin from CSCaCO$_3$NP. Among the three mathematical models, the Higuchi kinetic release best fit the release kinetic of Cur-CSCaCO$_3$NP. Thus, it can be deduced that the release kinetic of Cur-CSCaCO$_3$NP was due to the effect of diffusion rate and slow degradation of cockle shell nanomaterial. This could be possible because Higuchi equation model describes the release kinetics as consequences of dissolution and diffusion rates [69]. In respect to this, the mechanism of curcumin release from the mesoporous surface and layered matrix of CSCaCO$_3$NP involves the simultaneous penetration of pH medium, dissolution of curcumin and gradual leaching out of curcumin through CSCaCO$_3$NP interstitial pores. CSCaCO$_3$NP poses numerous porosity with multiple layers [22]. Thus, Cur-CSCaCO$_3$NP in the respective pH medium initially releases curcumin via diffusion at a rate proportional to the square root of time before the gradual and complete degradation of Cur-CSCaCO$_3$NP for proper curcumin release. Hence, Cur-CSCaCO$_3$NP release mechanism obeyed the Higuchi model release manner. The Higuchi model of drug release from of curcumin from other nanoparticles were reported earlier by previous studies [38,39,70,71].

5. Conclusions

In the current study, spherical shaped CSCaCO$_3$NP were successfully synthesized using a low cost, environmental friendly and simple top down method. Conjugation of curcumin with CSCaCO$_3$NP with excellent loading capacity was also successful. Curcumin was encapsulated with a substantial release *in vitro* as shown in Figure 13. A slow and substantial release of curcumin from CSCaCO$_3$NP was observed at pH 1.2 compared to the rapid sustained release of curcumin at pH 7.4, suggesting that Cur-CaCO$_3$NP could hardly be released in the gastric medium. The release data were fitted well in Higuchi equation model indicating that the release of curcumin from CSCaCO$_3$NP was controlled by diffusion and slow degradation mechanism. Therefore, CSCaCO$_3$NP showed promising potentials in promoting bioavailability, stability and reducing the insolubility of free curcumin for effective oral delivery of curcumin towards successful therapeutic applications. Additionally, the *in vivo* practical application of the newly synthesized Cur-CaCO$_3$NP against lead induced cerebral damage in animal models is currently ongoing by the research team to evaluate the *in vivo* therapeutic efficacy of Cur-CSCaCO$_3$NP.

 doi:10.20944/preprints201908.0254.v1

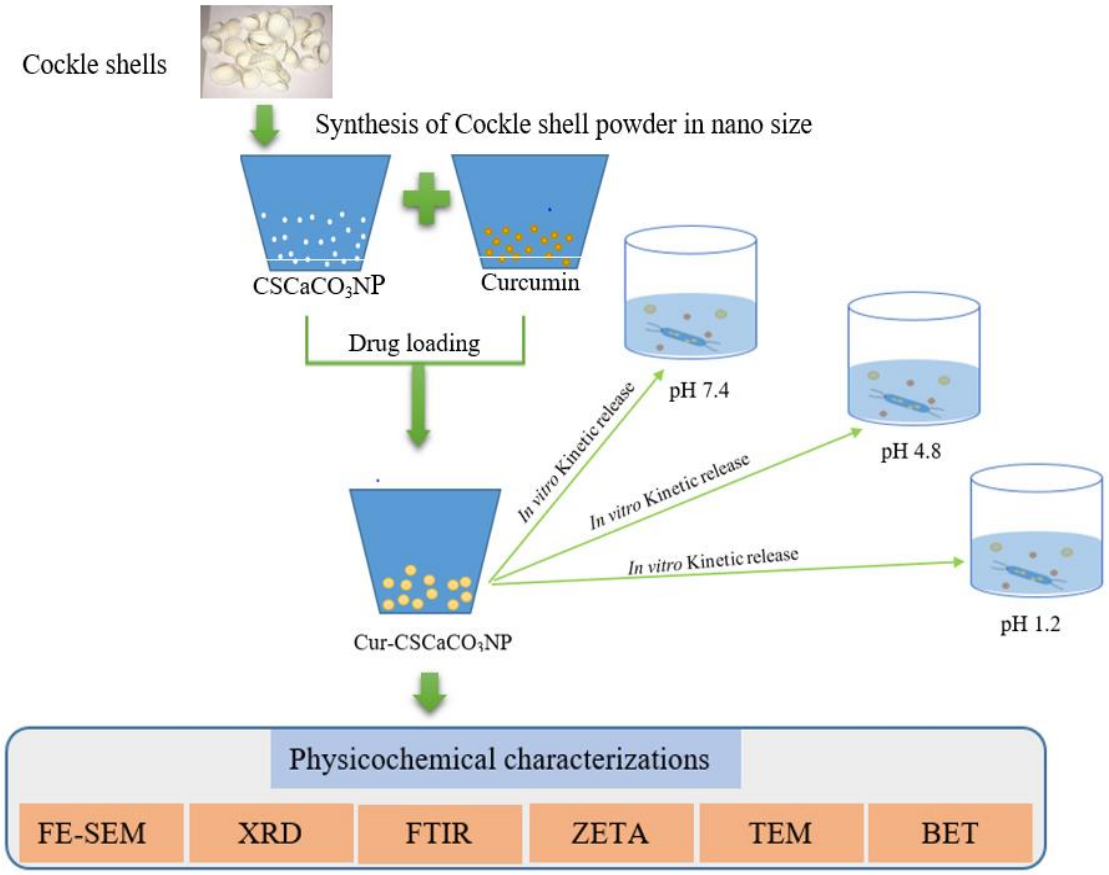

Figure 13. Diagrammatic representation of the synthesis, characterization and *in vitro* kinetic release mechanism of Cur-CSCaCO3NP

Author Contributions: "conceptualization, M.M.M.; M.A.M.M. and Z.A.B.Z.; methodology M.M.M.; A.D.; M.A.M.M.; E.B.A.R and Z.A.B.Z., validation, M.M.M.; A.D.; and Z.A.B.Z.; formal analysis M.M.M.; A.D. and M.A.M.M. investigation, M.M.M.; K.A.; A.D.; M.A.M.M.; and Z.A.B.Z.; data curation, M.M.M.; A.D; writing—original draft preparation, M.M.M.; writing—review and editing, M.M.M.; K.A.; A.D.; S.M.C.; supervision, E.B.A.R.; M.A.M.M.; Z.A.B.Z.

Abbreviations

CSCaCO3NP: Cockle shell calcium carbonate nanoparticles, Cur- CSCaCO3NP: Curcumin loaded-Cockle shell calcium carbonate nanoparticles, PDI: Polydispersity Index, IR: Immediate release, GIT: Gastrointestinal tracts, CaCO3: Calcium carbonate, XRD: X-ray diffractometer, BET; Brunauer-Emmett-teller, TEM: Transmission electron microscope, FT-IR: Fourier Transform Infrared Rays, FE-SEM: Field emission scanning electron microscope, EE%: Percentage encapsulation efficiency LE%: Percentage loading efficiency, BS-12: Dodecyl dimethyl betaine, BJH: Barrett-Joyner-halenda, hrs: Hours, μm: Micrometer.

Funding: This research was funded by Universiti Putra Malaysia, (Grant number GP-IPS 9663600).

Conflicts of Interest: The authors declare no conflict of interest.

 doi:10.20944/preprints201908.0254.v1

Appendix A

Drug loading

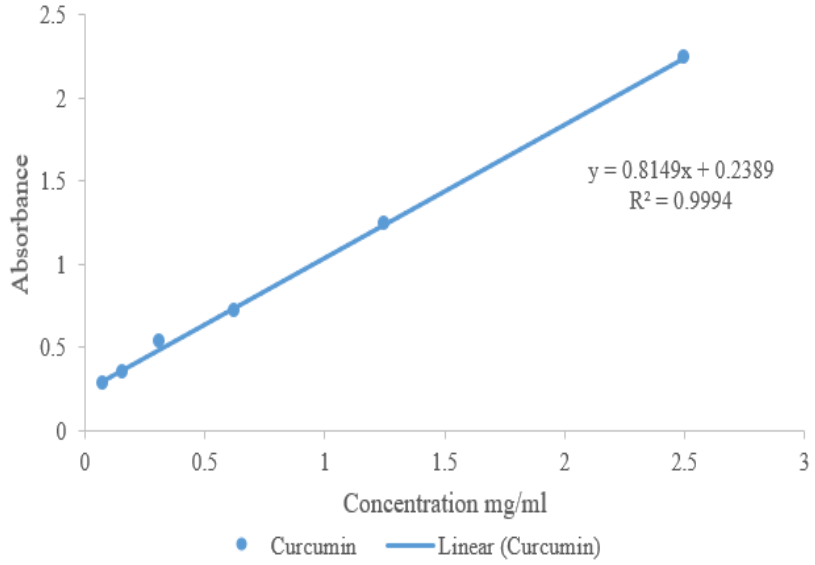

Figure A1. Standard calibration curve for absorbance verses different curcumin concentration

Appendix B

Table A1: *In vitro* Kinetic Release

pH 1.2	pH 4.8	pH 7.4
NaCl (2g)	0.1M citric acid (50.70)	PBS (8 g)
Concentrated Hcl (7 mL)	0.2M Na_2HPO_4 (49.30)	Deionized H_2O (800 mL)
Pepsin (3.2 g)		
Deionized H_2O (1000 mL)		

Different pH solutions used for the *in vitro* kinetic release

References

1. Stupp, S.I.; Braun, P. V. Molecular manipulation of microstructures: Biomaterials, ceramics, and semiconductors. *Science (80-.).* **1997**, *277*, 1242–1248.

2. Jain, A.; Jain, S.K. In vitro and cell uptake studies for targeting of ligand anchored nanoparticles for colon tumors. *Eur. J. Pharm. Sci.* **2008**, *35*, 404–416.

3. Islam, K.N.; Bakar, M.Z.B.A.; Noordin, M.M.; Hussein, M.Z. Bin; Rahman, N.S.B.A.; Ali, M.E. Characterisation of calcium carbonate and its polymorphs from cockle shells (Anadara granosa). *Powder Technol.* **2011**, *213*, 188–191.

4. Ma, L.; Zhao, G.; Fang, Y.; Dai, W.; Ma, N. Facile synthesis of mesoporous calcium carbonate particles with finger citron residue as template and their adsorption performances for Congo red. *Adsorpt. Sci. Technol.* **2018**, *36*, 872–887.

5. Giner-Casares, J.J.; Henriksen-Lacey, M.; Coronado-Puchau, M.; Liz-Marzán, L.M. Inorganic nanoparticles for biomedicine: where materials scientists meet medical research. *Mater. Today* **2016**, *19*, 19–28.

6. Mohd Abd Ghafar, S.L.; Hussein, M.Z.; Abu Bakar Zakaria, Z. Synthesis and Characterization of Cockle Shell-Based Calcium Carbonate Aragonite Polymorph Nanoparticles with Surface Functionalization. *J. Nanoparticles* **2017**, *2017*, 1–12.

7. Bhawana; Basniwal, R.K.; Buttar, H.S.; Jain, V.K.; Jain, N. Curcumin nanoparticles: Preparation, characterization, and antimicrobial study. *J. Agric. Food Chem.* **2011**, *59*, 2056–2061.

8. Ji, S.; Lin, X.; Yu, E.; Dian, C.; Yan, X.; Li, L.; Zhang, M.; Zhao, W.; Dian, L. Curcumin-Loaded Mixed Micelles: Preparation, Characterization, and in Vitro Antitumor Activity. *J. Nanotechnol.* **2018**, *2018*, 9.

9. Kumar, A.; Ahuja, A.; Ali, J.; Baboota, S. Curcumin-loaded lipid nanocarrier for improving bioavailability, stability and cytotoxicity against malignant glioma cells. *Drug Deliv.* **2016**, *23*, 214–229.

10. Sharma, R.A.; Gescher, A.J.; Steward, W.P. Curcumin: The story so far. *Eur. J. Cancer* **2005**, *41*, 1955–1968.

11. Toshihide Takagi, Chandrasekharan Ramachandran, Marival Bermejo, Shinji Yamashita§, Lawrence X. Yu‖, and G.L.A. A Provisional Biopharmaceutical Classification of the Top 200 Oral Drug Products in the United States, Great Britain, Spain, and Japan. *Mol. Pharm.* **2006**, *3*, 631–641.

12. Kawabata, Y.; Wada, K.; Nakatani, M.; Yamada, S.; Onoue, S. Formulation design for poorly water-soluble drugs based on biopharmaceutics classification system: Basic approaches and practical applications. *Int. J. Pharm.* **2011**, *420*, 1–10.

13. Hörter, D.; Dressman, J.. Influence of physicochemical properties on dissolution of drugs in the gastrointestinal tract1PII of original article: S0169-409X(96)00487-5. The article was originally published in Advanced Drug Delivery Reviews 25 (1997) 3–14.1. *Adv. Drug Deliv. Rev.* **2002**, *46*, 75–87.

14. Chen, A.-L.; C.-H., H.; J.-K., L.; M.-M., H.; Y.-F., H.; T.-S., S.; J.-Y., K.; J.-T., L.; B.-R., L.; M.-S., W.; et al.

Phase I clinical trial of curcumin, a chemopreventive agent, in patients with high-risk or pre-malignant lesions. *Anticancer Res.* **2001**, *21*, 2895–2900.

15. Anand, P.; Kunnumakkara, A.B.; Newman, R.A.; Aggarwal, B.B. Bioavailability of curcumin: Problems and promises. *Mol. Pharm.* **2007**, *4*, 807–818.

16. Marslin, G.; Prakash, J.; Qi, S.; Franklin, G. Oral delivery of curcumin polymeric nanoparticles ameliorates CCl4-induced subacute hepatotoxicity in wistar rats. *Polymers (Basel).* **2018**, *10*, 541.

17. Sahari, F.; Mijan, N.A. Cockle Shell As An Alternative Construction Material For Artificial Reef Faridah Sahari Email : sfaridah@faca.unimas.my Nurul Aniza Mijan Fakulti Seni Gunaan & Kreatif ,. **2011**.

18. Mailafiya, M.M.; Abubakar, K.; Danmaigoro, A.; Chiroma, S.M.; Bin, E.; Rahim, A.; Aris, M.; Moklas, M. Cockle Shell-Derived Calcium Carbonate (Aragonite) Nanoparticles : A Dynamite to Nanomedicine. *Appl. Sci.* **2019**, *9*, 2894.

19. Torchilin, V.P. Nanocarriers. *Pharm. Res.* **2007**, *24*, 2333–2334.

20. Jaji, A.Z.; Abu Bakar, M.Z. Bin; Mahmud, R.; Loqman, M.Y.; Hezmee, M.N.M.; Isa, T.; Wenliang, F.; Hammadi, N.I. Synthesis, characterization, and cytocompatibility of potential cockle shell aragonite nanocrystals for osteoporosis therapy and hormonal delivery. *Nanotechnol. Sci. Appl.* **2017**, *10*, 23–33.

21. Hoque, M.E. Processing and Characterization of Cockle Shell Calcium Carbonate (CaCO3) Bioceramic for Potential Application in Bone Tissue Engineering. *J. Mater. Sci. Eng.* **2014**, *02*, 2–6.

22. Danmaigoro, A.; Selvarajah, G.T.; Noor, M.H.M.; Mahmud, R.; Zakaria, M.Z.A.B. Development of cockleshell (Anadara granosa) derived CaCO3nanoparticle for doxorubicin delivery. *J. Comput. Theor. Nanosci.* **2017**, *14*, 5074–5086.

23. Fu, W.; Mohd Noor, M.H.; Yusof, L.M.; Ibrahim, T.A.T.; Keong, Y.S.; Jaji, A.Z.; Zakaria, M.Z.A.B. In vitro evaluation of a novel pH sensitive drug delivery system based cockle shell-derived aragonite nanoparticles against osteosarcoma. *J. Exp. Nanosci.* **2017**, 1–22.

24. Isa, T.; Zakaria, Z.A.B.; Rukayadi, Y.; Hezmee, M.N.M.; Jaji, A.Z.; Imam, M.U.; Hammadi, N.I.; Mahmood, S.K. Antibacterial activity of ciprofloxacin-encapsulated cockle shells calcium carbonate (Aragonite) nanoparticles and its biocompatability in macrophage J774A.1. *Int. J. Mol. Sci.* **2016**, *17*.

25. Hammadi, N.I.; Abba, Y.; Hezmee, M.N.M.; Razak, I.S.A.; Jaji, A.Z.; Isa, T.; Mahmood, S.K.; Zakaria, M.Z.A.B. Formulation of a Sustained Release Docetaxel Loaded Cockle Shell-Derived Calcium Carbonate Nanoparticles against Breast Cancer. *Pharm. Res.* **2017**, *34*, 1193–1203.

26. Hamidu, A.; Mokrish, A.; Mansor, R.; Shameha, I.; Razak, A.; Danmaigoro, A.; Jaji, A.Z.; Bakar, Z.A. Modi fi ed methods of nanoparticles synthesis in pH-sensitive nano-carriers production for doxorubicin delivery on MCF-7 breast cancer cell line. *Int. J. Nanomedicine* **2019**, *14*, 3615–3627.

27. Danmaigoro, A.; Selvarajah, G.T.; Mohd Noor, M.H.; Mahmud, R.; Abu Bakar, M.Z. Toxicity and Safety Evaluation of Doxorubicin-Loaded Cockleshell-Derived Calcium Carbonate Nanoparticle in Dogs. *Adv.*

Pharmacol. Sci. **2018**, *2018*.

28. Jaji, A.Z.; Zakaria, Z.A.B.; Mahmud, R.; Loqman, M.Y.; Hezmee, M.N.M.; Abba, Y.; Isa, T.; Mahmood, S.K. Safety assessments of subcutaneous doses of aragonite calcium carbonate nanocrystals in rats. *J. Nanoparticle Res.* **2017**, *19*, 175.

29. Montalbán, M.; Coburn, J.; Lozano-Pérez, A.; Cenis, J.; Víllora, G.; Kaplan, D. Production of Curcumin-Loaded Silk Fibroin Nanoparticles for Cancer Therapy. *Nanomaterials* **2018**, *8*, 126.

30. Karri, V.V.S.R.; Kuppusamy, G.; Talluri, S.V.; Mannemala, S.S.; Kollipara, R.; Wadhwani, A.D.; Mulukutla, S.; Raju, K.R.S.; Malayandi, R. Curcumin loaded chitosan nanoparticles impregnated into collagen-alginate scaffolds for diabetic wound healing. *Int. J. Biol. Macromol.* **2016**, *93*, 1519–1529.

31. Sanoj Rejinold, N.; Muthunarayanan, M.; Chennazhi, K.P.; Nair, S. V.; Jayakumar, R. Curcumin loaded fibrinogen nanoparticles for cancer drug delivery. *J. Biomed. Nanotechnol.* **2011**, *7*, 521–534.

32. Bisht, S.; Feldmann, G.; Soni, S.; Ravi, R.; Karikar, C.; Maitra, A.; Maitra, A. Polymeric nanoparticle-encapsulated curcumin ("nanocurcumin"): A novel strategy for human cancer therapy. *J. Nanobiotechnology* **2007**, *5*, 1–18.

33. Chirio, D.; Peira, E.; Dianzani, C.; Muntoni, E.; Gigliotti, C.; Ferrara, B.; Sapino, S.; Chindamo, G.; Gallarate, M. Development of Solid Lipid Nanoparticles by Cold Dilution of Microemulsions: Curcumin Loading, Preliminary In Vitro Studies, and Biodistribution. *Nanomaterials* **2019**, *9*, 230.

34. Athira, G.K.; Jyothi, A.N. Preparation and characterization of curcumin loaded cassava starch nanoparticles with improved cellular absorption. *Int. J. Pharm. Pharm. Sci.* **2014**, *6*, 171–176.

35. Islam, K.N.; Bakar, M.Z.B.A.; Ali, M.E.; Hussein, M.Z. Bin; Noordin, M.M.; Loqman, M.Y.; Miah, G.; Wahid, H.; Hashim, U. A novel method for the synthesis of calcium carbonate (aragonite) nanoparticles from cockle shells. *Powder Technol.* **2013**, *235*, 70–75.

36. Udompornmongkol, P.; Chiang, B.H. Curcumin-loaded polymeric nanoparticles for enhanced anti-colorectal cancer applications. *J. Biomater. Appl.* **2015**, *30*, 537–546.

37. Mofazzal Jahromi, M.A.; Al-Musawi, S.; Pirestani, M.; Fasihi Ramandi, M.; Ahmadi, K.; Rajayi, H.; Mohammad Hassan, Z.; Kamali, M.; Mirnejad, R. Curcumin-loaded Chitosan Tripolyphosphate Nanoparticles as a safe,natural and effective antibiotic inhibits the infection of Staphylococcusaureus and Pseudomonas aeruginosa in vivo. *Iran. J. Biotechnol.* **2014**, *12*, 1–8.

38. Anish H. Verma, T.S Sampath Kumar, K. Madhumathi, Y. Rubaiya, Murugan Ramalingan, and M.D. Curcumin Releasing Eggshell Derived Carbonated. *J. Nanosci. Nanotechnol.* **2019**, *19*, 6872–6880.

39. Kar, S.; Kundu, B.; Reis, R.L.; Sarkar, R.; Nandy, P.; Basu, R.; Das, S. Curcumin ameliorates the targeted delivery of methotrexate intercalated montmorillonite clay to cancer cells. *Eur. J. Pharm. Sci.* **2019**, *135*, 91–102.

40. Shaikh, J.; Ankola, D.D.; Beniwal, V.; Singh, D.; Kumar, M.N.V.R. Nanoparticle encapsulation improves

oral bioavailability of curcumin by at least 9-fold when compared to curcumin administered with piperine as absorption enhancer. *Eur. J. Pharm. Sci.* **2009**, *37*, 223–230.

41. Wang, C.; Liu, Y.; Bala, H.; Pan, Y.; Zhao, J.; Zhao, X.; Wang, Z. Facile preparation of CaCO3nanoparticles with self-dispersing properties in the presence of dodecyl dimethyl betaine. *Colloids Surfaces A Physicochem. Eng. Asp.* **2007**, *297*, 179–182.

42. Shafiu Kamba, A.; Ismail, M.; Tengku Ibrahim, T.A.; Zakaria, Z.A.B. A pH-sensitive, biobased calcium carbonate aragonite nanocrystal as a novel anticancer delivery system. *Biomed Res. Int.* **2013**, *2013*.

43. Maleki Dizaj, S.; Barzegar-Jalali, M.; Zarrintan, M.H.; Adibkia, K.; Lotfipour, F. Calcium carbonate nanoparticles as cancer drug delivery system. *Expert Opin. Drug Deliv.* **2015**, *12*, 1649–1660.

44. Ghaji, M.S.; Abu, Z.; Zakaria, B.; Shameha, A.R.I.; Noor, M.; Hezmee, M.; Hazilawati, H. Novelty to Synthesis Nanoparticles from Cockle Shall via Mechanical Method to Delivery and Controlled Release of Cytarabine. *J. Comput. Theor. Nanosci.* **2017**, *14*, 1–9.

45. Kiranda, H.K.; Mahmud, R.; Abubakar, D.; Zakaria, Z.A. Fabrication , Characterization and Cytotoxicity of Spherical-Shaped Conjugated Gold-Cockle Shell Derived Calcium Carbonate Nanoparticles for Biomedical Applications. *Nanoscale Res. Lett.* **2018**, *13*, 1–10.

46. Ghadi, A.; Mahjoub, S.; Tabandeh, F.; Talebnia, F. Synthesis and optimization of chitosan nanoparticles: Potential applications in nanomedicine and biomedical engineering. *Casp. J. Intern. Med.* **2014**, *5*, 156–161.

47. Kura, A.U.; Hussein, M.Z.; Fakurazi, S.; Arulselvan, P. Layered double hydroxide nanocomposite for drug delivery systems; bio-distribution, toxicity and drug activity enhancement. *Chem. Cent. J.* **2014**, *8*.

48. Bhatia, S. *Natural polymer drug delivery systems: Nanoparticles, plants, and algae*; 2016; ISBN 9783319411293.

49. Priyadarsini, K.I. The chemistry of curcumin: From extraction to therapeutic agent. *Molecules* **2014**, *19*, 20091–20112.

50. Render, D.; Samuel, T.; King, H.; Vig, M.; Jeelani, S.; Babu, R.J.; Rangari, V. Biomaterial-Derived Calcium Carbonate Nanoparticles for Enteric Drug Delivery. *J. Nanomater.* **2016**, *2016*.

51. Kamba, S.A.; Ismail, M.; Hussein-Al-Ali, S.H.; Ibrahim, T.A.T.; Zakaria, Z.A.B. In vitro delivery and controlled release of doxorubicin for targeting osteosarcoma bone cancer. *Molecules* **2013**, *18*, 10580–10598.

52. Md Enamul Hoque, M.S.; Islam, and K.M.N. Processing and Characterization of Cockle Shell Calcium Carbonate (CaCO3) Bioceramic for Potential Application in Bone Tissue Engineering. *J. Mater. Sci. Eng.* **2014**, *02*, 2–6.

53. Jiang, W.; Kim, B.Y.S.; Rutka, J.T.; Chan, W.C.W. Nanoparticle-mediated cellular response is size-dependent. *Nat. Nanotechnol.* **2008**, *3*, 145–150.

54. Verma, A.; Stellacci, F. Effect of surface properties on nanoparticle-cell interactions. *Small* **2010**, *6*, 12–21.

55. Gendelman, H.E.; Anantharam, V.; Bronich, T.; Ghaisas, S.; Jin, H.; Kanthasamy, A.G.; Liu, X.; McMillan, J.E.; Mosley, R.L.; Narasimhan, B.; et al. Nanoneuromedicines for degenerative, inflammatory, and infectious nervous system diseases. *Nanomedicine Nanotechnology, Biol. Med.* **2015**, *11*, 751–767.

56. A. Abel Lozano-Pérez, Ana L. Gil, Sergio A. Pérez, Natalia Cutillas, Hajo Meyer, Mónica Pedreño, Salvador Aznar-Cervantes, Christoph Janiak, Jose Luis Cenis, and J.R. Silk fibroin nanoparticles: Efficient vehicles for the natural antioxidant quercetin. *Int. J. Pharm.* **2017**, *25*, 11–19.

57. Supakorn Boonyuen; Monta Malaithong; Apisit Prokaew Decomposition study of calcium carbonate in shell. *Thai J. Sci. Technol.* **2015**, *4*, 115–122.

58. Linga Raju, C.; Narasimhulu, K. V.; Gopal, N.O.; Rao, J.L.; Reddy, B.C.V. Electron paramagnetic resonance, optical and infrared spectral studies on the marine mussel Arca burnesi shells. *J. Mol. Struct.* **2002**, *608*, 201–211.

59. Duan, J.; Mansour, H.M.; Zhang, Y.; Deng, X.; Chen, Y.; Wang, J.; Pan, Y.; Zhao, J. Reversion of multidrug resistance by co-encapsulation of doxorubicin and curcumin in chitosan/poly(butyl cyanoacrylate) nanoparticles. *Int. J. Pharm.* **2012**, *426*, 193–201.

60. Pandit, R.S.; Gaikwad, S.C.; Agarkar, G.A.; Gade, A.K.; Rai, M. Curcumin nanoparticles: physico-chemical fabrication and its in vitro efficacy against human pathogens. *3 Biotech* **2015**, *5*, 991–997.

61. Rachmawati, H.; Yanda, Y.L.; Rahma, A.; Mase, N. Curcumin-loaded PLA nanoparticles: Formulation and physical evaluation. *Sci. Pharm.* **2016**, *84*, 191–202.

62. Karri, V.V.S.R.; Kuppusamy, G.; Talluri, S.V.; Mannemala, S.S.; Kollipara, R.; Wadhwani, A.D.; Mulukutla, S.; Raju, K.R.S.; Malayandi, R. Curcumin loaded chitosan nanoparticles impregnated into collagen-alginate scaffolds for diabetic wound healing. *Int. J. Biol. Macromol.* **2016**, *93*, 1519–1529.

63. Wang, W.; Zhu, R.; Xie, Q.; Li, A.; Xiao, Y.; Li, K.; Liu, H.; Cui, D.; Chen, Y.; Wang, S. Enhanced bioavailability and efficiency of curcumin for the treatment of asthma by its formulation in solid lipid nanoparticles. *Int. J. Nanomedicine* **2012**, *7*, 3667–3677.

64. Jain, D.; Banerjee, R. Comparison of ciprofloxacin hydrochloride-loaded protein, lipid, and chitosan nanoparticles for drug delivery. *J. Biomed. Mater. Res. - Part B Appl. Biomater.* **2008**, *86*, 105–112.

65. Chen, X.; Zou, L.Q.; Niu, J.; Liu, W.; Peng, S.F.; Liu, C.M. The stability, sustained release and cellular antioxidant activity of curcumin nanoliposomes. *Molecules* **2015**, *20*, 14293–14311.

66. Shao, P.; Xuan, S.; Wu, W.; Qu, L. International Journal of Biological Macromolecules Encapsulation ef fi ciency and controlled release of Ganoderma lucidum polysaccharide microcapsules by spray drying using different combinations of wall materials. *Int. J. Biol. Macromol.* **2019**, *125*, 962–969.

67. Khan, A.; Mehdi, S.H.; Ahmad, I.; Rizvi, M.M.A. International Journal of Biological Macromolecules Characterization and anti-proliferative activity of curcumin loaded chitosan nanoparticles in cervical

963 cancer. *Int. J. Biol. Macromol.* **2016**, *93*, 242–253.

964 68. Gillies, E.R.; Fréchet, J.M.J. Dendrimers and dendritic polymers in drug delivery. *Drug Discov. Today*
965 **2005**, *10*, 35–43.

966 69. Paul, D.R. Elaborations on the Higuchi model for drug delivery. *Int. J. Pharm.* **2011**, *418*, 13–17.

967 70. Gautam Singhvi, M.S. In-vitro drug release characterization models. *Int. J. Pharm. Stud. Res.* **2011**, *II*, 77–
968 84.

969 71. Rezaei, A.; Nasirpour, A. Evaluation of Release Kinetics and Mechanisms of Curcumin and Curcumin-
970 β-Cyclodextrin Inclusion Complex Incorporated in Electrospun Almond Gum/PVA Nanofibers in
971 Simulated Saliva and Simulated Gastrointestinal Conditions. *Bionanoscience* **2019**, *9*, 438–445.

972